Plant Science 226 (2014) 147–161

Contents lists available at ScienceDirect

Plant Science

journal homepage: www.elsevier.com/locate/plantsci

Impacts of rising tropospheric ozone on photosynthesis and metabolite levels on field grown soybean

Jindong Sun[a,*], Zhaozhong Feng[a,1], Donald R. Ort[a,b]

[a] Institute for Genomic Biology, University of Illinois, Urbana, IL 61801, United States
[b] Global Change and Photosynthesis Research Unit, USDA/ARS, University of Illinois, Urbana, IL 61801, United States

ARTICLE INFO

Article history:
Available online 20 June 2014

Keywords:
Ozone
Soybean
Crop yield
Photosynthesis
Metabolites

ABSTRACT

The response of leaf photosynthesis and metabolite profiles to ozone (O_3) exposure ranging from 37 to 116 ppb was investigated in two soybean cultivars Dwight and IA3010 in the field under fully open-air conditions. Leaf photosynthesis, total non-structural carbohydrates (TNC) and total free amino acids (TAA) decreased linearly with increasing O_3 levels in both cultivars with average decrease of 7% for an increase in O_3 levels by 10 ppb. Ozone interacted with developmental stages and leaf ages, and caused higher damage at later reproductive stages and in older leaves. Ozone affected yield mainly *via* reduction of maximum rate of Rubisco carboxylation (V_{cmax}) and maximum rates of electron transport (J_{max}) as well as a shorter growing season due to earlier onset of canopy senescence. For all parameters investigated the critical O_3 levels (~50 ppb) for detectable damage fell within O_3 levels that occur routinely in soybean fields across the US and elsewhere in the world. Strong correlations were observed in O_3-induced changes among yield, photosynthesis, TNC, TAA and many metabolites. The broad range of metabolites that showed O_3 dose dependent effect is consistent with multiple interaction loci and thus multiple targets for improving the tolerance of soybean to O_3.

1. Introduction

Tropospheric ozone concentrations ([O_3]) are more than twice what they were a century ago in the middle latitudes of the Northern Hemisphere and portend a significant threat to food and feed production as [O_3] continues to rise over coming decades [1,2]. Intergovernmental Panel on Climate Change (IPCC) Assessment Report Five (AR5) indicates that [O_3] could rise 20–25% between 2015 and 2050, and further increase by 40–60% by 2100 if current emission trends continue [3].

The accumulated doses of O_3 exposure above a "critical O_3 level" (*e.g.* 40 ppb) introduced by UNECE or the dose actually taken up into the plants above the "critical O_3 flux level" have been used to determine and predict O_3 damage to vegetation [4,5]. It is generally observed that crop growth and yield change little with O_3 levels below the "critical O_3 level" but decrease linearly with O_3 levels above the "critical O_3 level" [6,7]. However, the "critical O_3 level" is mostly based on enclosure studies such as growth chambers, glasshouses or open top chambers where the atmosphere–vegetation coupling may be very different from field conditions. In various parts of the world, crops already frequently experience [O_3] above the "critical O_3 level" of 40 ppb. Nearly one-quarter of the earth's land surface is currently at risk from tropospheric O_3 in excess of 60 ppb during mid-summer, with even greater concentrations occurring in isolated regions [8,9], with

Abbreviations: *%D*, fraction of absorbed radiation dissipated in the antenna; *%P*, fraction of absorbed radiation utilized in PSII photochemistry; *%X*, fraction of absorbed radiation by PSII neither used in photochemistry nor dissipated in the PSII antennae; α, leaf absorbance; β, fraction of absorbed quanta reaching PSII; Φ_{PSII}, quantum efficiency of PSII; *A*, net rate of CO_2 uptake per unit of projected leaf area; A_o, light-saturated CO_2 assimilation rates at [C_i] equals ambient [CO_2]; A_c, Rubisco-limited photosynthesis; A_j, RuBP-limited photosynthesis; A_{sat}, light-saturated CO_2 assimilation rates at ambient [CO_2]; AOT40, accumulated exposure dose over threshold 40 ppb; ANOVA, analysis of variance; Chiro, chiro-inositol; Chl, chlorophyll; C_i, intercellular CO_2 concentration; C_{itr}, transition C_i between A_c and A_j; [CO_2], CO_2 concentration; C_x, carotenoids; DOY, day of the year; ETR, electron transport rate; FACE, free air concentration enrichment; F'_m, maximal fluorescence for a light-adapted leaf; F'_o, minimal fluorescence for a light-adapted leaf; F_s, steady-state fluorescence for a light-adapted leaf; F'_v/F'_m, ratio of variable fluorescence to maximal fluorescence for a light-adapted leaf; Fru, fructose; Glc, glucose; g_m, mesophyll conductance; g_s, stomatal conductance; J_{max}, maximum rate of electron transport; *I*, stomatal limitation; Myo, myo-inositol; Pin, pinitol; PPFD or Q, photosynthetic photon quantum flux density; *qP*, quenching of photochemical efficiency of PSII; R_d, mitochondrial respiration rate in the light; SLW, specific leaf weight; Suc, sucrose; SUM06, sum of hourly average [O_3] above or equal 0.06 ppm; TAA, total amino acids; TNC, total non-structural carbohydrates; V_{cmax}, maximum rate of Rubisco carboxylation.

* Corresponding author. Current address: DuPont Pioneer, Johnston, IA 50131, United States. Tel.: +1 515 535 4995; fax: +1 515 535 3444.
E-mail addresses: jindong.sun@gmail.com, jindong.sun@pioneer.com (J. Sun).
[1] Current address: State Key Laboratory of Urban and Regional Ecology, Research Center for Eco-Environmental Sciences, Chinese Academy of Sciences, Beijing 100085, China.

http://dx.doi.org/10.1016/j.plantsci.2014.06.012
0168-9452/

Western Europe, the mid-west and eastern United States, and eastern China being exposed to some of the highest background levels [3,7].

Soybean, the most important legume and 4th most important seed crop in the world, is among the most O_3-sensitive crops and showed yield decrease at O_3 levels as low as 40 ppb [4,10]. SoyFACE (Soybean Free Air Concentration Enrichment) facility was used to elevate surface O_3 levels under completely open-air conditions in the field. Ozone containing air was ejected just above crop canopy to elevate O_3 levels. Previous studies at SoyFACE showed that a small increase in O_3 levels (20% increase over ambient O_3 levels) caused seed yield loss by ~10% [11–14]. Earlier leaf senescence and decreased photosynthesis in late grain filling appear to drive the O_3-induced losses in primary production and seed yield [12]. A 20% increase in surface O_3 levels did not significantly alter photosynthetic capacity of newly expanded leaves, but as these leaves aged, losses in photosynthetic carbon assimilation occurred in leaves formed during reproductive stage [14]. The leaf position in crop canopy may cause the differences between the two types of leaves as the leaves formed during reproductive stage are in the upper of the canopy and exposed to O_3 levels higher than the leaves formed in vegetative stage due to O_3 gradient across the canopy (O_3 levels decrease from top to bottom of the canopy). A recent SoyFACE study employing a range of above ambient [O_3] showed a dose dependent linearly decrease in soybean yield, photosynthesis, and altered antioxidant capacity [15]. The work reported here expands on that O_3 dose experiment.

The quantitative responses of leaf sugars and amino acids to various O_3 levels are not well defined although they may hold the key to understanding the underlying mechanism of O_3 effects in soybean and other C3 plants. Previous reports showed that elevated O_3 can cause changes in plant metabolites and allocation of carbon and energy resources, but the exact responses and mechanisms are yet to be elucidated. It was reported that elevated O_3 increased sugars including sucrose, glucose and fructose contents in birch [16], but decreased total non-structural carbohydrates (TNC) in soybean [15]. Elevated O_3 increased the gene expressions of antioxidant metabolism [17,18], antioxidant content [19] and antioxidant capacity [15]. It has also been reported that elevated O_3 can increase secondary metabolites from polyamine biosynthesis pathway such as GABA, from phenylpropanoid metabolic pathway, and stress hormones such as ethylene and ABA (for review, see [20]).

In this study the responses of two soybean cultivars (Dwight and IA3010) to elevated O_3 levels were investigated under 9 O_3 levels ranging from 37 up to 116 ppb and at various developmental stages and leaf ages in SoyFACE under field conditions. The objectives were to determine (1) how developmental stages and leaf age as well as their interactions impacted the physiological responses; (2) the quantitative relationships of various physiological responses with O_3 levels and thus the critical O_3 threshold; (3) the physiological factors responsible for the deleterious effects of ozone on photosynthesis and crop productivity.

2. Materials and methods

2.1. Ozone treatment and experimental design

The study was conducted in 2009 at the SoyFACE facility (Champaign, IL, see Ort et al. [11] for details). The field was managed according to standard regional agronomic practice for annual corn/soybean rotation. No nitrogen fertilizer was added. Plants at all treatment levels were capable of N_2 fixation. Soybean seeds [*Glycine max* (L.) Merr.] were planted on June 10 in nine 20-m diameter plots fumigated with various O_3 concentrations from early vegetative stage (end of June) to maturity (end of September). The daily 9-h average O_3 concentrations from June 15 (seedling emergence) to end of September (105 days) were 37 (ambient), 40, 46, 54, 58, 71, 89, 95 and 116 ppb (Fig. 1). Several soybean cultivars were planted in 0.38 m rows in each plot of which Dwight and IA3010 cultivars were sampled at R1 (DOY 208), R2 (DOY 222), R4 (DOY 236) and R5 (DOY 250) stages for this study. Three young leaves (the youngest fully expanded leaves) and three old leaves (2 nodes down from the youngest fully expanded leaves) were selected at random for each cultivar in each block for gas exchange and subsequent measurements.

2.2. AOT40 and SUM06

The accumulated O_3 doses over a threshold of 40 ppb (AOT40) and the sums of hourly O_3 average greater than or equal to 0.06 ppm (SUM06) were calculated based on hourly means for 9 h daily across the whole growing season (105 days) and corrected to 3-month standard (90 days) introduced by UNECE [5,6].

2.3. Gas exchange

Gas exchange was measured using portable gas exchange systems (LI-COR 6400LCF; LI-COR, Lincoln, NE) as described previously [21]. The CO_2 sensors and water vapor sensors of the gas exchange systems were calibrated using gas of a known [CO_2] with 21% oxygen and nitrogen as balance, and known water vapor concentrations generated with a controlled humidification system (LI-610 Portable Dew Point Generator; LI-COR). Leaf temperatures were set at 25 °C and PPFD levels were controlled using a chamber integrated red-blue light source with 10% blue light for all of the measurements. The relative humidity was maintained between 60% and 70% in the leaf chamber. After steady-state CO_2 and water vapor exchange were achieved at 400 μbar [CO_2] and PPFD of 1500 μmol m^{-2} s^{-1}. The responses of A to C_i were measured at PPFD 1500 μmol m^{-2} s^{-1} with [CO_2] starting at 400 μbar surrounding the leaf, and [CO_2] was decreased stepwise to 50 μbar [CO_2]. The [CO_2] was then set again to 400 μbar and increased stepwise to 1500 μbar. Each individual A/C_i curve consisted of 10 individual measurements at various [CO_2] levels (400, 200, 100, 50, 400, 600, 800, 1000, 1200 and 1500 μbar) and took approximately 40 min to complete. The responses of A to PPFD were measured at 400 μbar [CO_2] and PPFD from 2000 to 0 μmol m^{-2} s^{-1} in 10 steps (2000, 1500, 1000, 500, 250, 200, 150, 100, 50, 0).

2.4. Determination of V_{cmax}, J_{max}, R_d, l and QY

The maximum carboxylation capacity (V_{cmax}), the maximum capacity for electron transport rate (J_{max}) and mitochondrial respiration in the light (R_d) were calculated from A/C_i curves using Farquhar's model as described previously [21,22,25], and using the temperature dependent kinetic parameters of Rubisco [23]. In this study, the third phase for A/C_i was not obvious, and thus, addition of TPU to the model did not affect the V_{cmax} and J_{max} estimates, that is, calculations with a two- or three-segment fitting model gave similar results. A custom-designed macro is used to calculate the transition C_i (C_{itr}) automatically using Farquhar's biochemical model [24]. Ethier's method was used to determine the effect of g_m on V_{cmax} [25]. Stomatal limitation (l) was calculated as $(A_o - A_{sat})/A_o \times 100$, where A_o was calculated based on V_{cmax} and R_d. The curves were using a non-rectangular hyperbola least square curve fitting procedure to estimate the maximum apparent quantum yield (QY) [26].

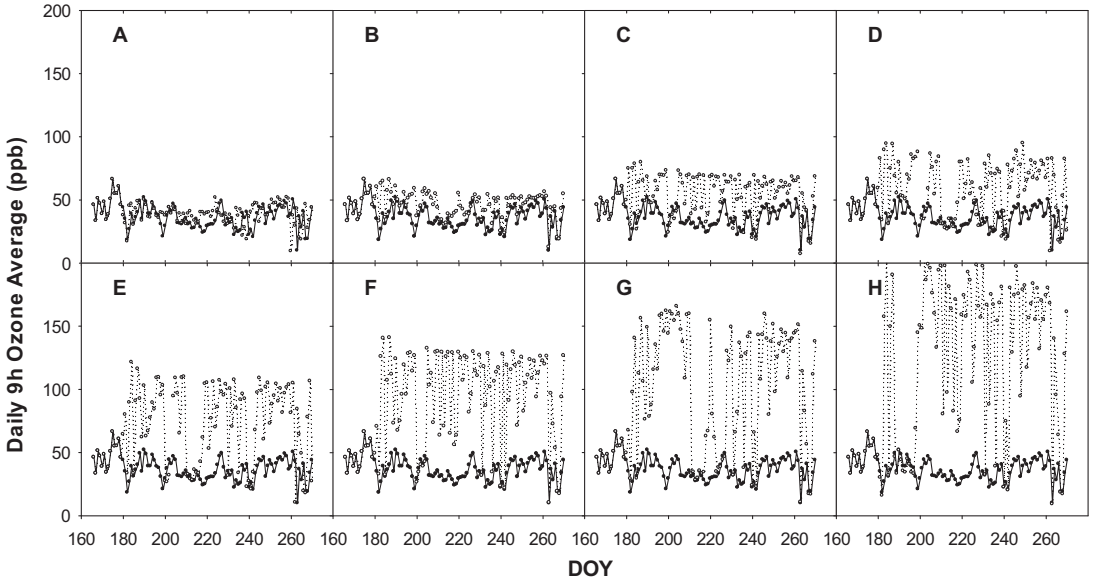

Fig. 1. Daily 9-h average ozone concentrations across the growing season for the ambient ozone concentration (closed circles, overall average 37 ± 10 ppb) and various elevated ozone treatments (open circles). The overall average ozone concentrations for various elevated ozone treatments were 40 ± 9 ppb (A), 46 ± 10 ppb (B), 54 ± 16 ppb (C), 58 ± 21 ppb (D), 71 ± 30 ppb (E), 89 ± 37 ppb (F), 95 ± 49 ppb (G) and 116 ± 64 ppb (H).

2.5. Chlorophyll fluorescence

Chlorophyll fluorescence was measured simultaneously with gas exchange using portable gas exchange systems with integrated chlorophyll fluorescence chamber (LI-6400LCF, LI-COR, Lincoln, NE) as described previously [21]. The actual photochemical efficiency of PSII in the saturated light (F'_v/F'_m) was calculated as $(F'_m - F'_o)/F'_m$, quenching of photochemical efficiency of PSII (qP) was calculated as $(F'_m - F_s)/(F'_m - F'_o)$, and the quantum yield of non-cyclic electron transport (Φ_{PSII}) was calculated as $(F'_m - F_s)/F'_m$ and ETR was calculated as $(\Phi_{PSII} \times PPFD \times \alpha \times \beta)$, where α, the light absorbed by the leaf, was assumed to be 0.87, and β, the factor for the partitioning of photons between incident PSII and PSI, was assumed to be 0.5 [21,27]. The fraction of absorbed radiation dissipated in the antenna (%D) and utilized in PSII photochemistry (%P) were estimated as $(1 - (F'_v - F'_m)) \times 100$ and $(F'_v - F'_m)\, qP \times 100$, respectively. The fraction of absorbed radiation by PSII neither used in photochemistry nor dissipated in the PSII antennae (%X) was estimated as $(F'_v - F'_m)\,(1 - qP) \times 100$ [28].

2.6. Estimation of mesophyll conductance

Estimates of mesophyll conductance (g_m) were calculated by the variable J method [29] and using the values of Γ^* at a given temperature from [30]. The g_m was constrained to 30 since a wide range of g_m values could satisfy the equations when it was large to infinite [29]. Mesophyll conductance (g_m) was solved using A, C_i and R_d calculated from gas exchange measurements, and rates of electron transport, J, measured using chlorophyll fluorescence. Gas exchange data measured at ambient [CO_2] were used for the g_m calculation as g_m varies with C_i [31].

2.7. Leaf pigment content

Leaf samples (1 cm^2) were extracted in 2 ml Eppendorf tubes with 1 ml of 95% ethanol in the dark at 4 °C for a couple of days until leaf discs were colorless. Chlorophyll (Chl) a and b and carotenoids (C_x) were determined by measuring the absorbance at 470, 648.6, and 664.2 nm with a microplate spectrophotometer (Biotek, Winooski, VT) using the extinction coefficients as described in [32].

2.8. Leaf size (LA)

The leaf areas were estimated from digital images of young and old trifoliate leaves with Image-J software (Research Service Branch, NIH).

2.9. Determination of starch, sucrose, glucose and fructose by coupled enzymes

Leaf discs (~2 cm^2) were taken at mid-day on sunny days and extracted with 80% (v/v) ethanol several times until the leaf discs were colorless. The ethanol soluble fractions from each sample were pooled and frozen at −20 °C until analyzed for sugars and amino acids. The leaf residue was homogenized in a microcentrifuge tube for 2 min with 2 tungsten beads inside with a tissue lyser at maximum frequency (30) (TissueLyser, Qiagen, Valencia, CA). The homogenate was combined with a 0.2-ml of 0.5 mM KOH and heated for 30 min at 95 °C with a heating block. The pH was adjusted to approximately 5.5 by the addition of 0.2 ml of 1 M acetic acid. Each of the samples was incubated with amyloglucosidase (10 units in a sample volume of 0.4 ml) at 55 °C for 2 h (tests showed no additional sugars were released beyond 2 h). Free sugars were determined spectrophotometrically in each extract by the coupled enzyme methods as previously described [21,33].

2.10. Sugar profiling using GC/MS

Sugar content was determined by GC/MS as described previously [34]. Individual standard stock solutions were prepared in 70% ethanol. Various amounts of the individual standard solutions were used to prepare calibration curves ranging from 0.3–75 μg in the autosample vials, and a composite standard was also prepared, varying from 50 to 150 nmol (1–40 μg). The aliquots were dried in the 1.5 ml autosampler vials in a Speed Vac-concentrator at 55 °C under vacuum and then converted to their oxime derivatives using the solution of pyridine containing

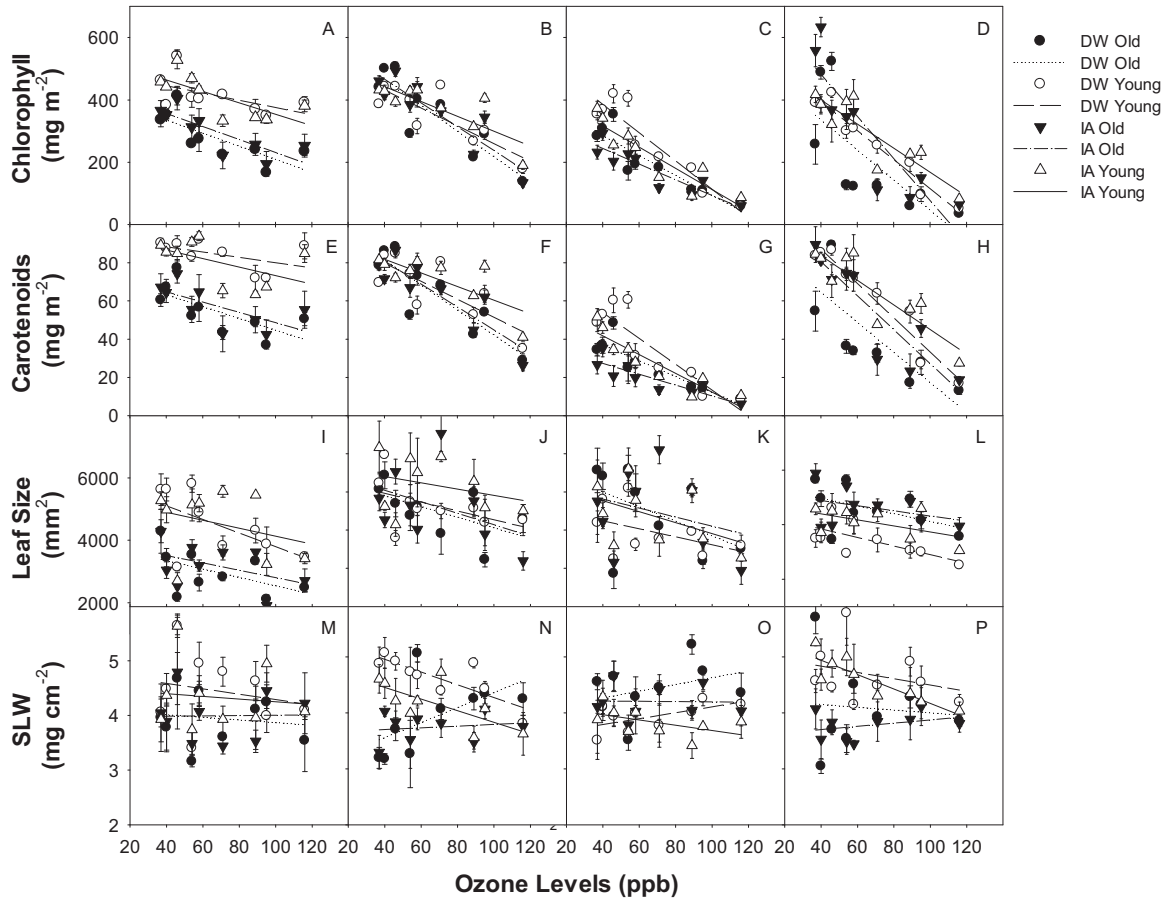

Fig. 2. Leaf total chlorophyll (Chl, A–D), carotenoids (C_x, E–H), leaf size (I–L) and specific leaf weight (SLW, M–P) for the young leaves (open symbol) and old leaves (closed symbol) of the 2 cultivars (DW, circle; IA, triangle) under various ozone levels and developmental stages – R1 (A, E, I and M), R2 (B, F, J and N), R4 (C, G, K and O) and R5 (D, H, L and P). Linear regressions were fit for DW old (dotted line), DW young (dashed line), IA old (dot dash line) and IA young leaves (solid line), respectively. The overall relationships of Chl, C_x and leaf size with mean [O_3] (x) can be described as $y = -3.38x + 526.0$, $y = -0.506x + 89.2$, and $y = -13.534x + 5672.5$, respectively. The overall R^2 values of Chl, C_x and leaf size with mean [O_3] were significant ($p < 0.0001$).

12.5 mg/ml hydroxylamine hydrochloride and 90 μg/ml phenyl-beta-D-glucopyranoside. Phenyl-beta-D-glucopyranoside was used as the internal standard. Hydroxylamine converted carbonyl compounds (aldehydes and ketones, such as fructose and glucose) to their oxime derivatives to prevent the anomerization thus reducing the number of peaks for simplicity. Samples were mixed by vortex and incubated at 70 °C for 40 min with occasional mixing. After cooling, hexamethyldisilazane (HMDS) was added after which the samples were allowed to react for 60 min at room temperature. Trifluoroacetic acid (TFA) was used in this method to remove any traces of water in the sample as HMDS is sensitive to water vapor. HMDS selectively silylates only carbohydrates to convert into their TMS–sugar derivatives, thus providing simpler chromatograms than BSTFA.

TMS–sugar derivatives were separated on a DB-1701 capillary column (30 m × 0.25 mm I.D., with a 0.25 μm film thickness, Supelco) using an Agilent 6890N gas chromatograph system and detected with Agilent 5975B insert MS detector (Agilent Technologies Inc, Santa Clara, CA). Compound identification was performed by comparison with the chromatographic retention characteristics and mass spectra of authentic standards, reported mass spectra and the NIST mass spectral library of the GC/MS data system with Agilent Chem Station program. Standard mixture of the known reference compounds were run side by side with the soybean samples each day. Compounds were quantified using total ion current (TIC) peak area, and converted to compound mass using calibration curves of external standards and internal standard.

2.11. Amino acid profiling using GC/MS

Derivatization of free AAs was accomplished using the EZ:faast free amino acid analysis kit (Phenomenex, Torrance, CA) and processed according to the manufacture's instructions. The processed samples were then analyzed by GC/MS for AA profiling. Compound identification was performed by comparison with the chromatographic retention characteristics and mass spectra of authentic standards, reported mass spectra and the mass spectral library of the GC/MS data system. Standard mixture of the known reference compounds were run side by side with the soybean samples each day. Compounds were quantified using total ion current (TIC) peak area, and converted to compound mass using calibration curves of external standards and internal standard.

2.12. Statistical analysis

All measured parameters influenced by cultivars, O_3 concentrations, leaf ages and developmental stages were analyzed by use of SAS ANOVA and the means and standard errors were calculated by use of SAS MEANS (SAS System 9.1; SAS Institute, Cary, N.C.). Significant probability values were set at $p < 0.05$.

Table 1
ANOVA of the effects of ozone levels (O), cultivars (V), leaf ages (A) and developmental stages (S) on the investigated variables.

	V	O	A	S	V × O	V × A	V × S	O × A	O × S	A × S
%D	<0.0001	<0.0001	0.0052	<0.0001	<0.0001	ns	ns	ns	<0.0001	0.0123
%P	ns	<0.0001	<0.0001	<0.0001	<0.0001	ns	<0.0001	0.0074	<0.0001	<0.0001
%X	<0.0001	<0.0001	<0.0001	<0.0001	0.0366	0.0212	ns	0.0113	0.0005	<0.0001
A_{max}	0.0342	<0.0001	<0.0001	N/A	0.0204	ns	N/A	ns	N/A	N/A
A_{sat}	ns	<0.0001	<0.0001	<0.0001	<0.0001	ns	<0.0001	0.005	<0.0001	<0.0001
Chiro-inositol[a]	ns	<0.0001	<0.0001	N/A	0.0015	ns	N/A	ns	N/A	N/A
Chl	<0.0001	<0.0001	<0.0001	<0.0001	<0.0001	0.0007	<0.0001	<0.0001	<0.0001	<0.0001
C_i	<0.0001	<0.0001	<0.0001	<0.0001	0.001	0.0002	0.0208	<0.0001	0.0017	<0.0001
Citr	ns	<0.0001	<0.0001	<0.0001	ns	ns	ns	0.0191	ns	0.0408
Citrate[a]	<0.0001	<0.0001	<0.0001	N/A	0.0076	0.0002	N/A	0.0191	N/A	N/A
C_x	ns	<0.0001	<0.0001	<0.0001	<0.0001	0.0174	<0.0001	<0.0001	<0.0001	<0.0001
ETR	ns	<0.0001	<0.0001	<0.0001	<0.0001	0.0486	<0.0001	0.002	<0.0001	<0.0001
Fructose	<0.0001	<0.0001	0.0007	<0.0001	0.0007	ns	<0.0001	0.0014	<0.0001	0.0017
F'_v/F'_m	<0.0001	<0.0001	0.0064	<0.0001	<0.0001	ns	ns	ns	<0.0001	0.0123
Glucose	<0.0001	0.0003	<0.0001	<0.0001	0.0005	ns	0.0007	0.0002	<0.0001	ns
g_m	ns	<0.0001	<0.0001	<0.0001	0.0029	ns	ns	ns	ns	ns
g_s	<0.0001	<0.0001	0.0031	<0.0001	<0.0001	0.0082	<0.0001	0.0068	0.0004	<0.0001
J_{max}	ns	<0.0001	<0.0001	<0.0001	0.0232	ns	0.0487	ns	0.0324	<0.0001
L	0.0036	<0.0001	<0.0001	<0.0001	ns	0.0016	ns	0.0039	0.0013	<0.0001
Leaf size	<0.0001	<0.0001	0.0096	<0.0001	<0.0001	0.0057	ns	ns	<0.0001	<0.0001
Malate[a]	<0.0001	<0.0001	<0.0001	N/A	ns	0.047	N/A	0.0003	N/A	N/A
Maltose[a]	0.0011	<0.0001	<0.0001	N/A	<0.0001	0.0068	N/A	0.002	N/A	N/A
Myo-inositol[a]	<0.0001	<0.0001	<0.0001	<0.0001	<0.0001	<0.0001	N/A	ns	N/A	N/A
SLW	ns	<0.0001	<0.0001	<0.0001	<0.0001	ns	0.0888	0.0007	0.0059	0.0001
PhiPSII	ns	<0.0001	<0.0001	<0.0001	<0.0001	ns	<0.0001	0.0077	<0.0001	<0.0001
Pinitol[a]	ns	<0.0001	<0.0001	N/A	ns	ns	N/A	0.048	N/A	N/A
qP	0.0036	<0.0001	<0.0001	<0.0001	<0.0001	0.0717	<0.0001	0.0017	<0.0001	<0.0001
QY[a]	ns	<0.0001	0.004	N/A	0.012	ns	N/A	ns	N/A	N/A
R_d	ns	ns	0.007	0.0005	ns	ns	ns	ns	ns	ns
Starch	<0.0001	<0.0001	<0.0001	<0.0001	0.0181	ns	ns	<0.0001	<0.0001	<0.0001
Sucrose	0.0017	<0.0001	<0.0001	<0.0001	ns	ns	ns	0.0248	<0.0001	<0.0001
V_{cmax}	ns	<0.0001	<0.0001	<0.0001	<0.0001	ns	ns	0.0007	0.0059	0.0001

N/A, not applicable; ns, not significant.
[a] Measured at R5 stage only.

3. Results

3.1. Ozone exposure

The daily 9-h average O_3 concentrations (mean [O_3]) in nine treatments across the whole growing season (105 days, from mid of June to end of September) were 37 (ambient), 40, 46, 54, 58, 71, 89, 95 and 116 ppb (Figs. 1 and S1). AOT40 over the same period in nine treatments was 2.7 (ambient), 3.7, 8.9, 17.2, 21.5, 32.2, 48.9, 55.0 and 74.9 ppm h (Fig. S1A). The AOT40 of 90 days values are shown in Fig. S1B. SUM06 was 1.16 (ambient), 1.2, 5.9, 35.1, 37.6, 50.1, 70.6, 74.2 and 95.2 ppm h for 105 days (Fig. S1A and 90 day values given in Fig. S1B). AOT40 and SUM06 and the mean [O_3] were highly correlated. The determination coefficients (R squares) between mean [O_3] and AOT40 was 0.998–0.999 and between mean [O_3] and SUM06 was 0.962–0.966.

3.2. Leaf pigments and senescence

The plants grown under O_3 levels of 116 ppb were senescent 1 week earlier than the plants grown under ambient control. DW plants were senescent 3–5 days earlier than IA plants. Leaf total chlorophyll (Chl) and carotenoids (C_x) decreased with O_3 levels (Fig. 2, Tables 1 and S1–S4). Chl decreased by 6.4% and C_x by 5.7% for each 10 ppb increase in mean [O_3]. The rates of decrease in Chl and C_x were higher in later developmental stages than in the earlier developmental stages (Table S4, $p < 0.05$). Young leaves had higher Chl and C_x than old leaves (Table S3, $p < 0.05$). The overall average Chl and C_x were 13% and 20% lower in old leaves than in the young leaves. Overall IA had 5% higher Chl and 2% higher C_x than DW (Table S2, $p < 0.05$).

3.3. Leaf size (LA) and specific leaf weight (SLW)

Leaf size decreased with O_3 levels (Fig. 2, Tables 1 and S1–S4). The overall average leaf size was 5% larger in IA than in DW. SLW was 8% larger for the young leaves than the old leaves but was not affected by O_3. SLW was not significantly different between the two cultivars.

3.4. CO_2 assimilation and stomata limitation

Light-saturated photosynthesis (A_{sat}) decreased with O_3 levels and developmental stages and was higher in young leaves than in the old leaves (Fig. 3, Tables 1 and S1–S4). The overall A_{sat} decreased by 7% per 10 ppb increase in O_3 levels. A_{sat} decreased 3% in R2, 12% in R4 and 31% in R5 stages compared to R1 stage. The overall average A_{sat} was 28% lower in the old leaves than in the young leaves. A_{sat} was not significantly different between the two cultivars.

The overall stomatal conductance (g_s) decreased by 6% per 10 ppb increase in O_3 levels (Fig. 3, Tables 1 and S1–S4). g_s decreased 7% in R2, 14% in R4 and 35% in R5 stages compared to R1 stage. g_s was 14% lower in IA than in DW. Stomatal limitation (l) was significantly affected by O_3 levels, leaf ages and developmental stages and varied between the two cultivars. Stomatal limitation (l) decreased by 9% per 10 ppb increase in ozone levels (Fig. 3, Tables 1 and S1–S4). Stomatal limitation (l) increased 21% in R2, 30% in R4 and 52% R5 stages compared to the R1 stage. The overall average l was 13% higher in IA than in DW. Despite the stomatal closure C_i increased with ozone levels. C_i was 11% higher in the old leaves than in the young leaves and was 4% lower in IA than in DW.

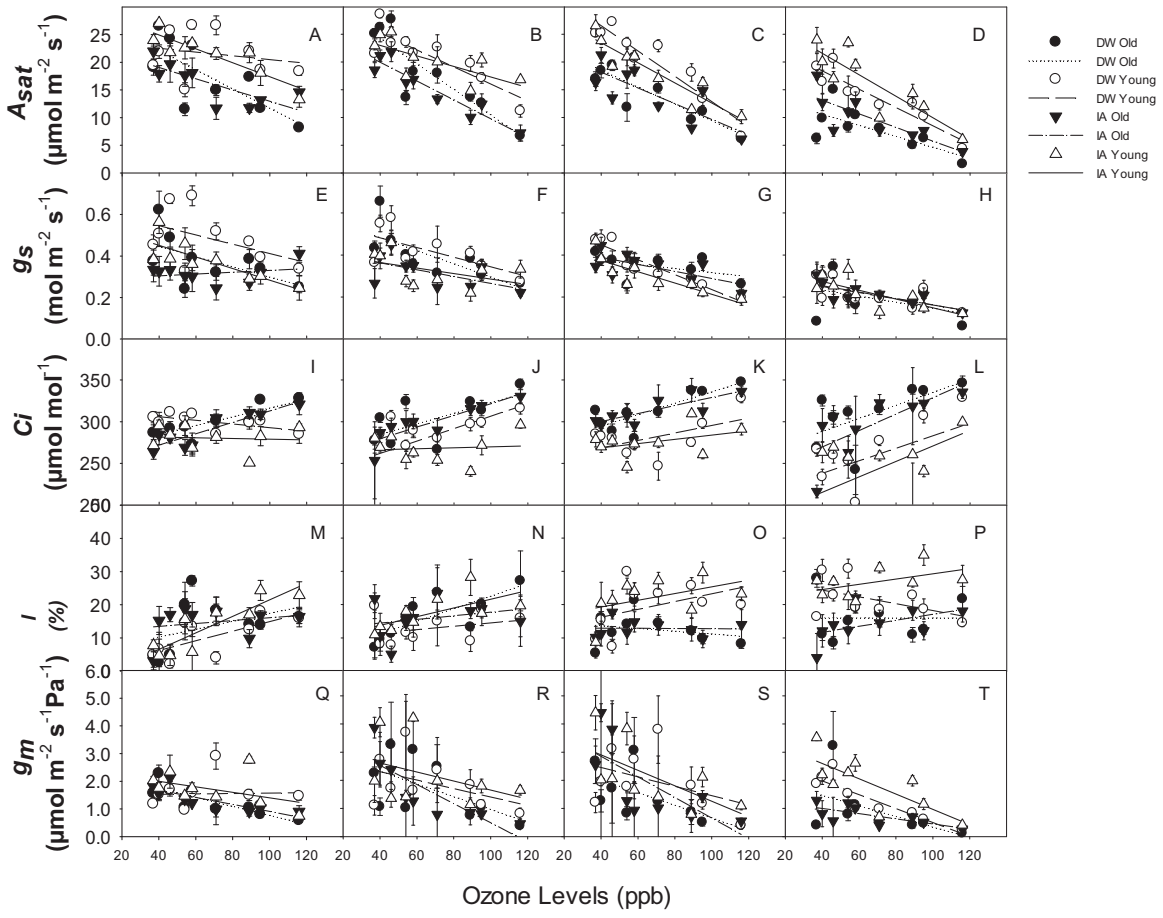

Fig. 3. A_{sat} (A–D), g_s (E–H), C_i (I–L), I (M–P) and g_m (Q–T) for the young leaves (open symbol) and old leaves (closed symbol) of the 2 cultivars (DW, circle; IA, triangle) under various ozone levels and developmental stages – R1 (A, E, I, M and Q), R2 (B, F, J, N and R), R4 (C, G, K, O and S) and R5 (D, H, L, P and T). Linear regressions were fit for DW old (dotted line), DW young (dashed line), IA old (dot dash line) and IA young leaves (solid line), respectively. The overall relationships of A_{sat}, g_s, C_i, I and g_m with mean [O_3] (x) can be described as $y = -0.152x + 27$, $y = -0.0021x + 0.4752$, $y = 0.406x + 267$ and $y = 0.077x + 11$, and $y = -0.02x + 2.86$, respectively. The overall R^2 values of A_{sat}, g_s, C_i, I and g_m with mean [O_3] were significant ($p < 0.001$).

3.5. Mesophyll conductance

Mesophyll conductance (g_m) decreased with O_3 levels and was lower in old leaves than in young leaves. The overall average g_m was 27% lower in the old leaves than in the young leaves (Fig. 3, Tables 1 and S1–S4).

3.6. Rubisco, maximum rate of electron transport, respiration and quantum yield

The maximum rates of Rubisco carboxylation (V_{cmax}) and the maximum rates of electron transport (J_{max}) were not significantly different between the two cultivars. The overall average V_{cmax} was 31% and J_{max} 28% lower in the old leaves than in the young leaves, respectively. V_{cmax} was similar between R1 and R2 stages and declined 11% in R4 and 29% in R5 stages. J_{max} was similar among R1, R2 and R4 stages and declined 16% in the R5 stage (Fig. 4, Tables 1 and S1–S4).

The rate of respiration in the light (R_d) was 19% lower in the old leaves than in the young leaves. R_d was not affected by O_3 levels, was not significantly different between the two cultivars and showed no clear pattern between R_d and developmental stages (Fig. 4, Tables 1 and S1–S4).

The transition intercellular [CO_2] (C_{itr}) increased 25% in R2, 20% in R4 and 52% in R5 stages compared to the R1 stage. C_{itr} was not significantly different between the two cultivars (Fig. 4, Tables 1 and S1–S4).

Quantum yield (QY) decreased with O_3 levels and was 12% lower in the old leaves than in the young leaves. QY was not significantly different between the two cultivars (Fig. 5, Tables 1 and S1–S4).

3.7. Leaf chlorophyll a fluorescence

The overall average F'_v/F'_m, PhiPSII and qP were 28%, 32% and 34% lower in the old leaves than in the young leaves, respectively. The ratio of variable fluorescence to maximal fluorescence (F'_v/F'_m) was similar among R1, R2 and R4 stages and declined slightly (3%) in the R5 stage. Quantum yield of PSII (PhiPSII) decreased 9% in R2, 19% in R4 and 31% in R5 stages compared to the R1 stage. Photochemical quenching (qP) decreased 5%, 22% and 30% in the R2, R4 and R5 stages compared to the R1 stage, respectively. F'_v/F'_m was not significantly different between the two cultivars. PhiPSII and qP were only marginally higher in DW than in IA (Fig. 6, Tables 1 and S1–S4).

The fraction of absorbed radiation utilized in PSII photochemistry (%P) decreased 9% in R2, 19% in R4 and 31% in R5 stages compared to the R1 stage. The overall average %P was 32% lower in the old leaves than in the young leaves. The fraction of absorbed radiation utilized in PSII photochemistry (%P) was not significantly different between the two cultivars (Fig. 7, Tables 1 and S1–S4). The

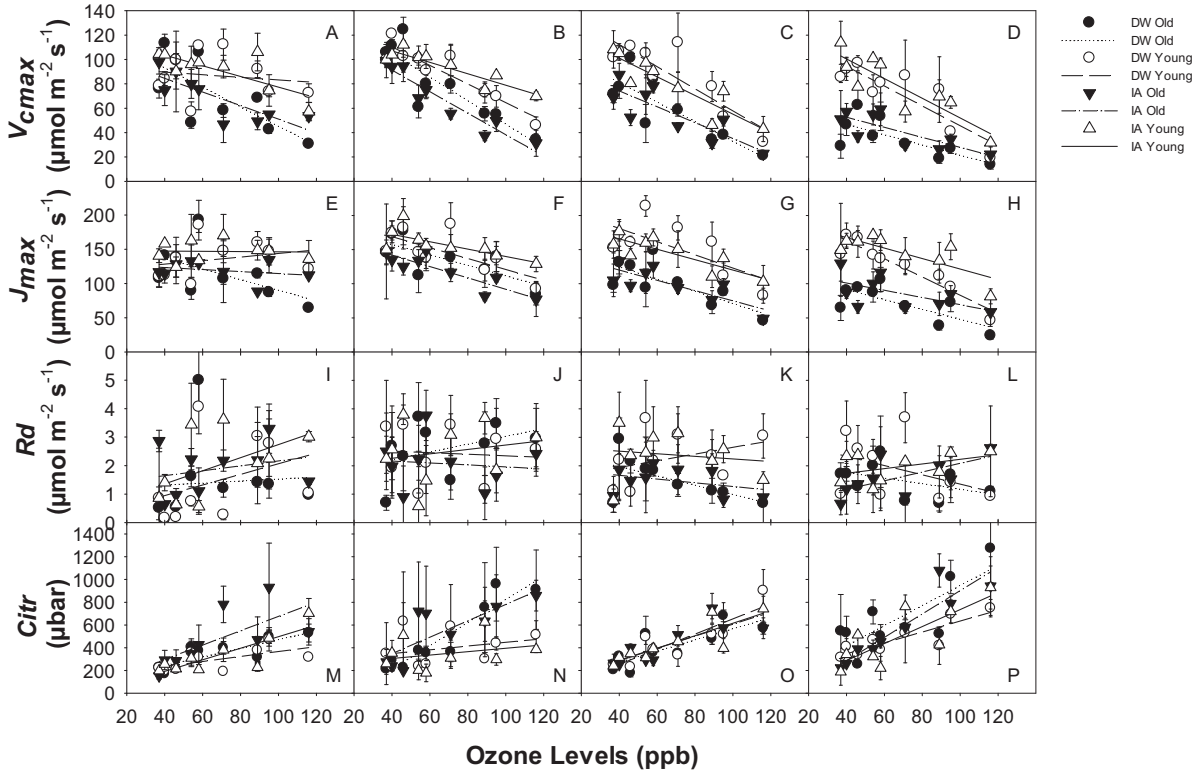

Fig. 4. V_{cmax} (A–D), J_{max} (E–H), R_d (I–L) and C_{itr} (M–P) for the young leaves (open symbol) and old leaves (closed symbol) of the 2 cultivars (DW, circle; IA, triangle) under various ozone levels and developmental stages – R1 (A, E, I and M), R2 (B, F, J and N), R4 (C, G, K and O) and R5 (D, H, L and P). Linear regressions were fit for DW old (dotted line), DW young (dashed line), IA old (dot dash line) and IA young leaves (solid line), respectively. The overall relationships of V_{cmax}, J_{max} and C_{itr} with mean [O_3] (x) can be described as $y = -0.65x + 116$, $y = -0.65x + 169$, and $y = 0.41x + 267$, respectively. The overall R^2 values of V_{cmax}, J_{max} and C_{itr} with mean [O_3] were significant ($p < 0.0001$).

fraction of absorbed radiation dissipated in the antenna (%*D*) and the fraction of absorbed radiation by PSII neither used in photochemistry nor dissipated in the PSII antennae (%*X*) increased with O_3 levels and was lower in young leaves than in old leaves and lower in IA than in DW (Fig. 7, Tables 1 and S1–S4).

3.8. Leaf non-structural carbohydrate levels

The overall average leaf starch decreased 8% per 10 ppb increase in O_3. Leaf starch decreased 32–33% in the R2 and R4 stages and 45% in the R5 stage compared with the R1 stage. The overall average leaf starch content was 60% lower in the old leaves than in the young leaves. Leaf starch was slightly higher in DW than in IA in R1, R2 and R4 stages but slightly lower in DW than in IA in the R5 stage (Fig. 8, Tables 1 and S1–S4).

Leaf sucrose, glucose and fructose did not change significantly with O_3 levels during early reproductive stages but decreased with O_3 levels during late reproductive stages and was lower in the old leaves than in the young leaves (Fig. 8, Tables 1 and S1–S4).

Leaf pinitol, chiro-inositol, myo-inositol, malate and maltose decreased whereas citrate increased significantly with O_3 levels (Fig. 9). The overall average leaf pinitol, chiro-inositol, myo-inositol, malate and maltose decreased by 6%, 8%, 2%, 6% and 5%, respectively, but leaf citrate increased by 24%, per 10 ppb increase in O_3.

3.9. Leaf free amino acids

The total free amino acids decreased with O_3 levels (Fig. 10). Asn, Asp and Glu, the major amino acids from primary nitrogen assimilation, decreased with O_3 levels. Ser and Gly, the amino acids from photorespiration pathway, were little affected by elevated O_3 levels. Phe, one of the 3 major aromatic amino acids from prechorismate pathway, decreased with O_3 levels. Tyr and Trp, the other 2 of the 3 major aromatic amino acids from the prechorismate pathway, were little affected by O_3. GABA and Pro, two amino acids induced by drought stress, decreased with O_3 levels. Ala, another one of the major free amino acids, decreased with O_3 levels. Other amino acids such as His, Thr, Ile, Leu, Lys, Met, Thr and Val changed little with O_3 levels.

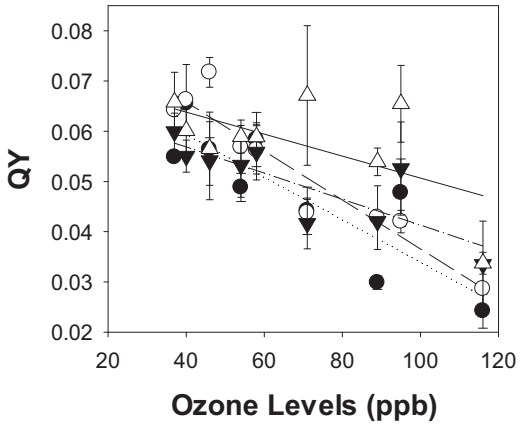

Fig. 5. QY for the young leaves (open symbol) and old leaves (closed symbol) of the 2 cultivars (DW, circle; IA, triangle) under various ozone levels at R5 stage. Linear regressions were fit for DW old (dotted line), DW young (dashed line), IA old (dot dash line) and IA young leaves (solid line), respectively. The overall relationship of QY with mean [O_3] (x) can be described as $y = -0.003x + 0.075$. The overall R^2 between QY and mean [O_3] was significant ($p < 0.0001$).

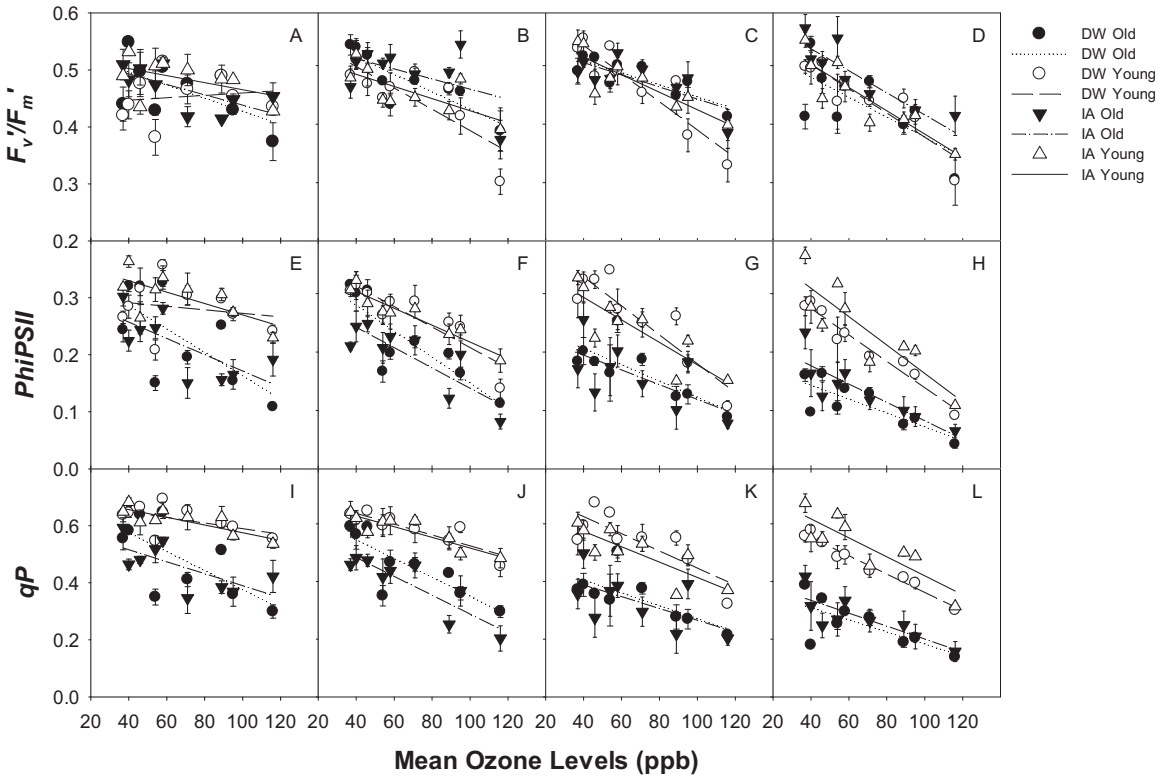

Fig. 6. F_v'/F_m' (A–D), *PhiPSII* (E–H) and *qP* (I–L) for the young leaves (open symbol) and old leaves (closed symbol) of the 2 cultivars (DW, circle; IA, triangle) under various ozone levels and developmental stages – R1 (A, E and I), R2 (B, F and J), R4 (C, G and K) and R5 (D, H and L). Linear regressions were fit for DW old (dotted line), DW young (dashed line), IA old (dot dash line) and IA young leaves (solid line), respectively. The overall relationships of F_v'/F_m', *PhiPSII* and *qP* with mean [O_3] (x) can be described as $y = -0.0013x + 0.552$, $y = -0.0016x + 0.329$, and $y = 0.0024x + 0.627$, respectively. The overall R^2 values of F_v'/F_m', *PhiPSII* and *qP* with mean [O_3] were significant ($p < 0.0001$).

4. Discussions

4.1. Differential down-regulation of photosynthetic components by elevated O_3 levels

Ozone sensitivity is associated with leaf characteristics related to the ability of O_3 to diffuse into the leaves and the ability of O_3 to diffuse through intercellular space into mesophyll cells [35,36]. Our results showed that g_s decreased whereas [C_i] and l increased with O_3 levels (Fig. 3, Tables 1 and S1–S4). These findings demonstrated that non-stomatal limitations mainly contributed to lower photosynthesis under elevated O_3. This conclusion confirms the previous hypothesis that decreased stomatal conductance is likely the result rather than the cause for photosynthesis reduction by O_3 [37,38].

The primary factor for non-stomatal limitation of photosynthesis was found to be V_{cmax} which decreased 6% for each 10 ppb ozone concentration increase, which accounted for ~85% of photosynthesis decrease under elevated O_3. This decrease in V_{cmax} due to elevated O_3 is consistent with the decrease in Rubisco gene expression [15] and the decrease in A_{sat} and with all chlorophyll fluorescence parameters including *qP*, F_v'/F_m', *PhiPSII*, *%P*, *%D* and *%X*.

Another non-stomatal limitation factor was g_m, which decreased by 8% for each 10 ppb increase in O_3 (Fig. 3, Table 2) that in turn caused 1% of decrease in V_{cmax} per 10 ppb O_3 increase (Fig. S2), which accounted for ~15% of photosynthesis decrease under elevated O_3. Our results showed that g_m decreased V_{cmax} by 17% on average, which agrees with the previous study that V_{cmax} would be 10–20% higher if g_m is assumed not limiting [23]. It is reported that some environmental conditions such as [CO_2] down-regulates g_m [31], but whether elevated O_3 affects g_m is not consistent. It is reported elevated O_3 causes either no change on g_m [39,40] or decrease in g_m [41,42]. Our results clearly show that ozone causes linear decrease in g_m. Different species and different methods for O_3 fumigation are likely the cause for the inconsistent effects of O_3 on g_m.

4.2. Differential effects of elevated O_3 on leaf metabolites

The majority of the sugars decreased under elevated O_3 levels (Figs. 8 and 9, Table 2). Sucrose and starch are the major primary metabolites from photosynthetically fixed carbon. On the one hand, reduction in sugar levels and synthesis rates of sugars and starch are the results of reduction in photosynthesis under elevated O_3 levels. On the other hand, reduction in rates of sucrose and starch synthesis would hence affect triose-p utilization and RuBP-regeneration limited photosynthesis. Triose-p utilization, mainly the rate of starch and sucrose synthesis, affects Pi recycle and hence RuBP regeneration [13,21,43]. Pinitol is one of the major sugars in soybean leaves (Fig. 9), contributing significantly to triose-p utilization. The function of pinitol in plants remains to be elucidated. It was reported that pinitol in plants was induced under drought stress and may act as protective compound such as osmolyte [44]. Lower levels of starch and sugars along with lower J_{max} and lower A_{sat} indicate that reduced rates of starch and sucrose synthesis and reduced triose-p utilization under elevated O_3 levels.

Citrate was the only one of the carbohydrates that showed an increase under elevated O_3 (Fig. 9). Higher pools of citrate may indicate higher anaplerotic reaction for TCA cycle for O_3 detoxification. It is reported that O_3 stimulates PEPC activity in common bean *Phaseolus vulgaris* [45] and *Pinus halepensis* [46]. In anaplerotic reaction PEP carboxylase catalyzes CO_2 fixation with PEP to produce oxaloacetate that can be subsequently reduced into malate and/or converted into citrate in TCA cycle. Such an increase could give rise

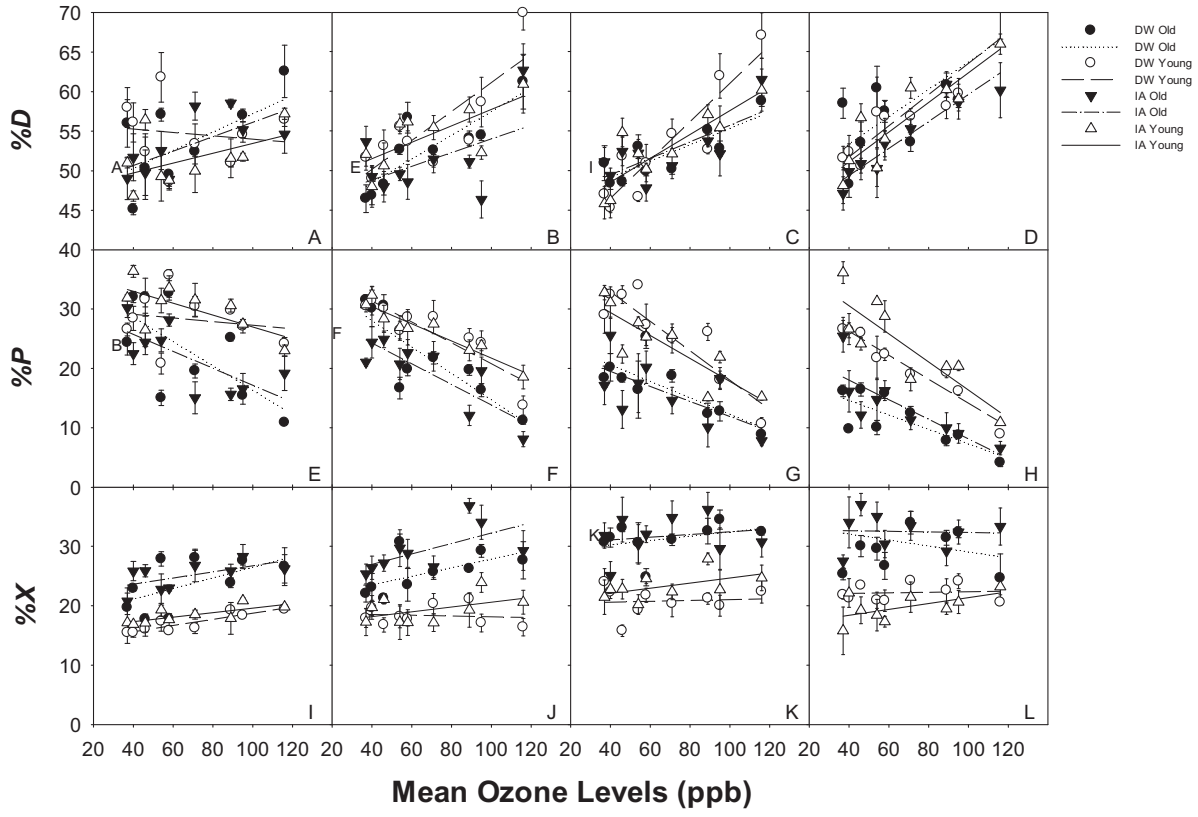

Fig. 7. %*D* (A–D), %*P* (E–H) and %*X* (I–L) for the young leaves (open symbol) and old leaves (closed symbol) of the 2 cultivars (DW, circle; IA, triangle) under various ozone levels and developmental stages – R1 (A, E and I), R2 (B, F and J), R4 (C, G and K) and R5 (D, H and L). Linear regressions were fit for DW old (dotted line), DW young (dashed line), IA old (dot dash line) and IA young leaves (solid line), respectively. The overall relationships of %*D*, %*P* and %*X* with mean [O_3] (*x*) can be described as $y = 0.13x + 44.8$, $y = -0.1626x + 32.9$, and $y = 0.0325x + 22.3$, respectively. The overall R^2 values of %*D*, %*P* and %*X* with mean [O_3] were significant ($p < 0.0001$).

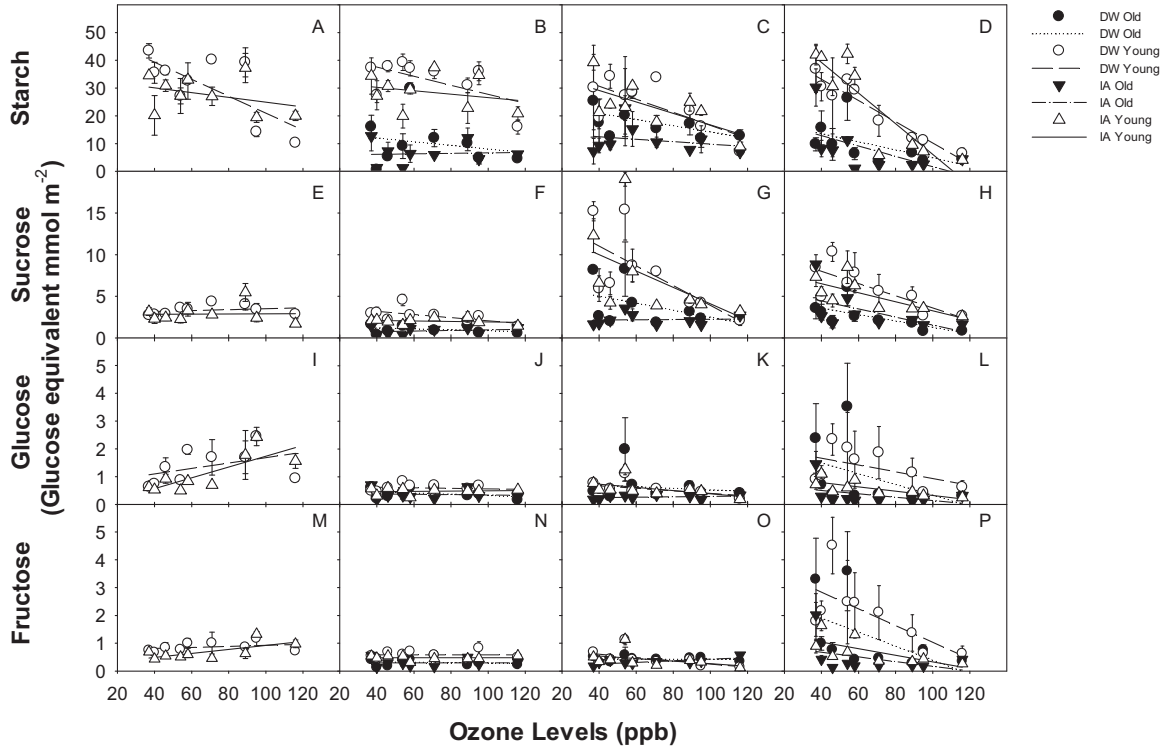

Fig. 8. Leaf starch (A–D), sucrose (E–H), glucose (I–L) and fructose (M–P) analyzed with enzymatic method for the young leaves (open symbol) and old leaves (closed symbol) of the 2 cultivars (DW, circle; IA, triangle) under various ozone levels and developmental stages – R1 (A, E, I and M), R2 (B, F, J and N), R4 (C, G, K and O) and R5 (D, H, L and P). Linear regressions were fit for DW old (dotted line), DW young (dashed line), IA old (dot dash line) and IA young leaves (solid line), respectively. The overall relationships of starch and sucrose with mean [O_3] (*x*) can be described as $y = -0.199x + 33.82$ and $y = -0.031x + 5.582$, respectively. The overall R^2 values of starch and sucrose with mean [O_3] were significant ($p < 0.0001$).

Table 2
Critical ozone levels estimated from Weibull fit and linear fit for various physiological variables with ozone levels at R5 stage.

Fit	Variable	Mean [O_3] (ppb)			AOT40 (ppm h)			SUM06 (ppm h)		
		Equation	R^2	Critical level[a]	Equation	R^2	Critical level[a]	Equation	R^2	Level[a]
Weibull	$\%P$	$1-\exp(-([O_3]/108.0488)^{1.833})$	0.329*	50	$1-\exp(-([AOT40]/65.5616)^{0.7446})$	0.320*	7	$1-\exp(-([SUM06]/119.9098)^{0.5699})$	0.267*	6
	A_{sat}	$1-\exp(-([O_3]/97.4697)^{1.9533})$	0.418*	49	$1-\exp(-([AOT40]/51.4123)^{0.8002})$	0.399*	7	$1-\exp(-([SUM06]/86.6603)^{0.6313})$	0.329*	5
	Chiro-inositol	$1-\exp(-([O_3]/80.2109)^{2.2385})$	0.544*	45	$1-\exp(-([AOT40]/34.2072)^{0.8682})$	0.542*	5	$1-\exp(-([SUM06]/56.3235)^{0.6149})$	0.452*	4
	Chl	$1-\exp(-([O_3]/90.3623)^{3.6656})$	0.547*	53	$1-\exp(-([AOT40]/41.919)^{1.6418})$	0.579*	11	$1-\exp(-([SUM06]/59.9187)^{1.9015})$	0.587*	18
	C_x	$1-\exp(-([O_3]/106.4835)^{4.3819})$	0.486*	65	$1-\exp(-([AOT40]/57.1652)^{2.1651})$	0.503*	20	$1-\exp(-([SUM06]/75.3114)^{2.7512})$	0.507*	33
	ETR	$1-\exp(-([O_3]/107.8974)^{1.7616})$	0.327*	50	$1-\exp(-([AOT40]/66.1248)^{0.7038})$	0.317*	7	$1-\exp(-([SUM06]/128.4957)^{0.5096})$	0.263*	6
	Fructose	$1-\exp(-([O_3]/82.3733)^{2.1539})$	0.141*	46	$1-\exp(-([AOT40]/35.6508)^{0.8561})$	0.135*	5	$1-\exp(-([SUM06]/58.4309)^{0.6089})$	0.103*	3
	F'_v/F'_m	$1-\exp(-([O_3]/157.7455)^{3.2349})$	0.415*	80	$1-\exp(-([AOT40]/117.4136)^{1.7182})$	0.418*	32	$1-\exp(-([SUM06]/127.6578)^{2.3153})$	0.421*	48
	Glucose	$1-\exp(-([O_3]/90.1607)^{1.8544})$	0.078*	47	$1-\exp(-([AOT40]/45.6685)^{0.6876})$	0.067*	5	$1-\exp(-([SUM06]/119.4780)^{0.3263})$	0.036*	4
	g_m	$1-\exp(-([O_3]/86.5461)^{2.0533})$	0.207*	46	$1-\exp(-([AOT40]/39.0248)^{0.8709})$	0.194*	6	$1-\exp(-([SUM06]/56.0945)^{1.1919})$	0.175*	9
	g_s	$1-\exp(-([O_3]/116.5321)^{1.6363})$	0.351*	51	$1-\exp(-([AOT40]/80.8438)0.65)$	0.324*	7	$1-\exp(-([SUM06]/168.6853)0.468)$	0.271*	6
	J_{max}	$1-\exp(-([O_3]/122.0565)^{3.6493})$	0.210*	68	$1-\exp(-([AOT40]/71.271)^{2.0965})$	0.206*	24	$1-\exp(-([SUM06]/87.0516)^{2.9664})$	0.208*	41
	Leaf size	$1-\exp(-([O_3]/367.5546)^{0.7472})$	0.120*	68	$1-\exp(-([AOT40]/4120.7)^{0.2361})$	0.091*	17	$1-\exp(-([SUM06]/944860.9)^{0.1188})$	0.050*	37
	Malate	$1-\exp(-([O_3]/110.4209)^{2.0251})$	0.392*	52	$1-\exp(-([AOT40]/66.4729)^{0.8679})$	0.285*	8	$1-\exp(-([SUM06]/84.4322)^{1.2058})$	0.244*	14
	Maltose	$1-\exp(-([O_3]/136.9072)^{2.9991})$	0.044*	68	$1-\exp(-([AOT40]/90.3578)^{1.5421})$	0.048*	21	$1-\exp(-([SUM06]/103.3911)^{2.2007})$	0.046	37
	Myo-inositol	$1-\exp(-([O_3]/190.8010)^{2.3124})$	0.057*	76	$1-\exp(-([AOT40]/107.5795)^{2.0112})$	0.046*	35	$1-\exp(-([SUM06]/113.0056)^{3.0835})$	0.042*	57
	PhiPSII	$1-\exp(-([O_3]/108.0488)1.833)$	0.329*	50	$1-\exp(-([AOT40]/65.5616)^{0.7446})$	0.320*	7	$1-\exp(-([SUM06]/119.9098)^{0.5699})$	0.267*	6
	Pinitol	$1-\exp(-([O_3]/116.4748)^{2.6109})$	0.219*	56	$1-\exp(-([AOT40]/65.8244)^{1.4927})$	0.211*	15	$1-\exp(-([SUM06]/80.2213)^{2.3762})$	0.199*	31
	qP	$1-\exp(-([O_3]/136.7757)^{1.4464})$	0.221*	53	$1-\exp(-([AOT40]/123.9426)^{0.5601})$	0.210*	8	$1-\exp(-([SUM06]/358.7302)0.375)$	0.168*	7
	QY	$1-\exp(-([O_3]/138.164)2.727)$	0.403*	66	$1-\exp(-([AOT40]/96.298)^{1.3642})$	0.398*	19	$1-\exp(-([SUM06]/107.436)1.923)$	0.405*	33
	Starch	$1-\exp(-([O_3]/78.2542)^{2.7786})$	0.360*	46	$1-\exp(-([AOT40]/32.4305)^{1.1759})$	0.356*	6	$1-\exp(-([SUM06]/50.1012)^{2.0198})$	0.310*	16
	Sucrose	$1-\exp(-([O_3]/94.3249)^{1.6585})$	0.235*	47	$1-\exp(-([AOT40]/51.0421)^{0.6064})$	0.206*	5	$1-\exp(-([SUM06]/127.5424)^{0.3262})$	0.190*	4
	V_{cmax}	$1-\exp(-([O_3]/107.236)^{1.8764})$	0.253*	50	$1-\exp(-([AOT40]/65.2676)^{0.7687})$	0.226*	7	$1-\exp(-([SUM06]/76.7549)^{1.3372})$	0.174*	14
Linear	$\%P$	$y=-0.1920[O_3]+30.433$	0.331*	49	$y=-0.2416[AOT40]+23.586$	0.327*	12	$y=-0.1712[SUM06]+23.526$	0.310*	15
	A_{sat}	$y=-0.1698[O_3]+24.42$	0.420*	48	$y=-0.2142[AOT40]+18.381$	0.417*	11	$y=-0.1519[SUM06]+18.33$	0.397*	13
	Chiro-inositol	$y=-0.0020[O_3]+0.241$	0.528*	45	$y=-0.0025[AOT40]+0.1696$	0.521*	9	$y=-0.0018[SUM06]+0.1699$	0.505*	10
	Chl	$y=-5.0681[O_3]+606.79$	0.587*	45	$y=-6.4274[AOT40]+427.46$	0.588*	9	$y=-4.8383[SUM06]+436.69$	0.623*	10
	C_x	$y=-0.8113[O_3]+111.56$	0.592*	47	$y=-1.0284[AOT40]+82.838$	0.592*	10	$y=-0.7524[SUM06]+83.557$	0.593*	12
	ETR	$y=-1.2572[O_3]+200.31$	0.329*	49	$y=-1.5818[AOT40]+155.48$	0.325*	12	$y=-1.1201[SUM06]+155.06$	0.307*	15
	Fructose	$y=-0.0181[O_3]+2.2929$	0.130*	46	$y=-0.0226[AOT40]+1.6476$	0.127*	9	$y=-0.0160[SUM06]+1.6419$	0.117*	11
	F'_v/F'_m	$y=-0.0019[O_3]+0.5786$	0.419*	64	$y=-0.0024[AOT40]+0.5108$	0.419*	23	$y=-0.0017[SUM06]+0.5101$	0.396*	31
	Glucose	$y=-0.0111[O_3]+1.5411$	0.077*	47	$y=-0.0138[AOT40]+1.1452$	0.075*	10	$y=-0.0090[SUM06]+1.1132$	0.058*	13
	g_m	$y=-0.0188[O_3]+2.444$	0.206*	46	$y=-0.0238[AOT40]+1.7795$	0.206*	10	$y=-0.0174[SUM06]+1.7921$	0.209*	11
	g_s	$y=-0.0023[O_3]+0.4079$	0.353*	51	$y=-0.0030[AOT40]+0.3243$	0.354*	13	$y=-0.0021[SUM06]+0.3247$	0.343*	16
	J_{max}	$y=-0.8516[O_3]+165.85$	0.195*	53	$y=-1.0792[AOT40]+135.71$	0.195*	15	$y=-0.7374[SUM06]+134.62$	0.171*	19
	Leaf size	$y=-12.625[O_3]+5029.9$	0.127*	73	$y=-15.824[AOT40]+4578.5$	0.124*	31	$y=-10.183[SUM06]+4539.6$	0.095*	45
	Malate	$y=-0.0126[O_3]+2.0204$	0.290*	49	$y=-0.0160[AOT40]+1.5714$	0.288*	12	$y=-0.0113[SUM06]+1.5696$	0.268*	15
	Maltose	$y=-0.0005[O_3]+0.097$	0.055*	53	$y=-0.0006[AOT40]+0.0787$	0.054*	15	$y=-0.0004[SUM06]+0.0782$	0.048*	20
	Myo-inositol	$y=-0.0007[O_3]+0.3915$	0.020	89	$y=-0.0009[AOT40]+0.3667$	0.019	43	$y=-0.0363[SUM06]+5.8237$	0.008	91
	PhiPSII	$y=-0.0019[O_3]+0.3043$	0.331*	49	$y=-0.0024[AOT40]+0.2359$	0.327*	12	$y=-0.0017[SUM06]+0.2353$	0.310*	15
	Pinitol	$y=-0.0427[O_3]+7.4171$	0.212*	51	$y=-0.0539[AOT40]+5.8994$	0.210*	13	$y=-0.0363[SUM06]+5.8237$	0.176*	17
	qP	$y=-0.0028[O_3]+0.5699$	0.222*	54	$y=-0.0036[AOT40]+0.4689$	0.219*	15	$y=-0.0025[SUM06]+0.4674$	0.205*	20
	QY	$y=-0.0003[O_3]+0.0752$	0.401*	58	$y=-0.0004[AOT40]+0.0631$	0.400*	18	$y=-0.0003[SUM06]+0.0632$	0.387*	22
	Starch	$y=-0.4074[O_3]+49.935$	0.344*	46	$y=-0.4098[AOT40]+26.806$	0.339*	9	$y=-0.2934[SUM06]+26.844$	0.321*	10
	Sucrose	$y=-0.0523[O_3]+7.6684$	0.234*	48	$y=-0.0653[AOT40]+5.7932$	0.228*	11	$y=-0.0439[SUM06]+5.6955$	0.190*	14
	V_{cmax}	$y=-0.6188[O_3]+98.536$	0.254*	49	$y=-0.7845[AOT40]+76.635$	0.254*	12	$y=-0.5465[SUM06]+76.17$	0.232*	15

* Significant at $p<0.01$.

[a] The critical ozone levels at which 10% decrease occurred in various physiological variables compared with the ambient ozone levels at developmental stage R5.

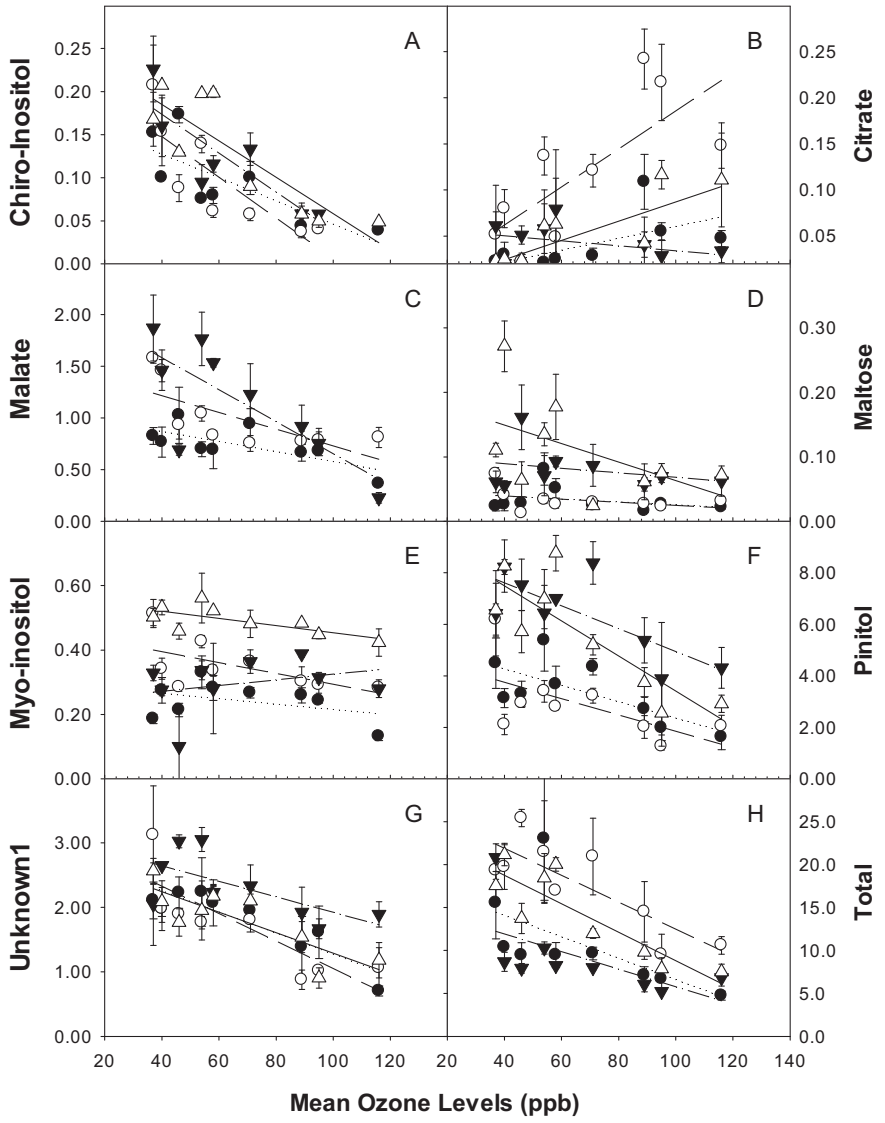

Fig. 9. Sugar profiling (unit = mmol m^{-2}) analyzed with GC/MS for the young leaves (open symbol) and old leaves (closed symbol) of the 2 cultivars (DW, circle; IA, triangle) under various ozone levels at R5 stage. Linear regressions were fit for DW old (dotted line), DW young (dashed line), IA old (dot dash line) and IA young leaves (solid line), respectively. The total soluble sugars (total, H) include all of the listed in this figure plus fructose, glucose and sucrose. The overall relationships of Chiro-inositol, citrate, malate, maltose, pinitol and total with mean [O_3] (x) can be described as $y = -0.002x + 0.241$, $y = 0.0009x + 0.004$, $y = -0.0126x + 2.02$, $y = -0.0005x + 0.097$, $y = -0.0427x + 7.42$ and $y = -0.1319x + 21.6$, respectively. The overall R^2 values of Chiro-inositol, citrate, malate, maltose, pinitol and total with mean [O_3] were significant ($p < 0.0001$).

to ATP and reducing power production by respiration to allow an enhancement of the constitutive detoxification systems activity in response to the release of reactive oxygen species (ROS) [47,48].

Most of the major free amino acids levels decreased significantly with O_3 levels, including Asn, Asp, Gln and Glu, which are the major amino acids from primary nitrogen assimilation likely indicating lower nitrogen assimilation in the O_3 grown soybean (Fig. 10). It is consistent with the reports that O_3 affected root growth [49], nitrogen uptake and nitrogen assimilation [50].

Tyr, Try and Phe are major aromatic amino acids from prechorismate pathway. Of the 3 major aromatic amino acids, Tyr and Trp were little affected by O_3 (Fig. 10). The accumulation of aromatic secondary metabolites is a known element of the plant defense response to O_3 and other stress, like lignins, wall-bound phenolics, phenolic acids, phytoalexins and flavonoids [51].

GABA and Pro are generally induced under drought and other stresses [52,53]. However, GABA and Pro decreased with O_3 levels, and did not accumulate under elevated O_3 levels (Fig. 10).

Future study on starch turnover (*e.g.* [21]), carbon partitioning (*e.g.* [27]), and metabolites fluxes (*e.g.* [54,55]) would provide more insights into the responses of metabolomics to elevated O_3.

4.3. The critical ozone levels that cause 10% damage vs. the ambient O_3 levels

The critical O_3 levels that cause 10% decrease varied among those measured parameters with average around 50 ppb for [O_3]. The estimated critical O_3 levels are between 48 and 49 ppb for photosynthesis such as A_{sat}, *ETR*, *PhiPSII* and V_{cmax}, between 45 and 47 ppb for photosynthetic pigments such as *Chl* and C_x, between 46 and 48 ppb for leaf major carbohydrates such as starch, sucrose, fructose and glucose, and 53 ppb for J_{max}. The critical O_3 levels that cause 10% decrease in seed yield compared to the ambient control are 49 ppb [15]. Photosynthetic pigments were the most sensitive parameter to O_3 among all variables measured. Ozone affects Rubisco-limited photosynthesis (*i.e.* V_{cmax}) more than RuBP-limited photosynthesis (*i.e.* J_{max}), indicating Rubisco is the early target of O_3 damage.

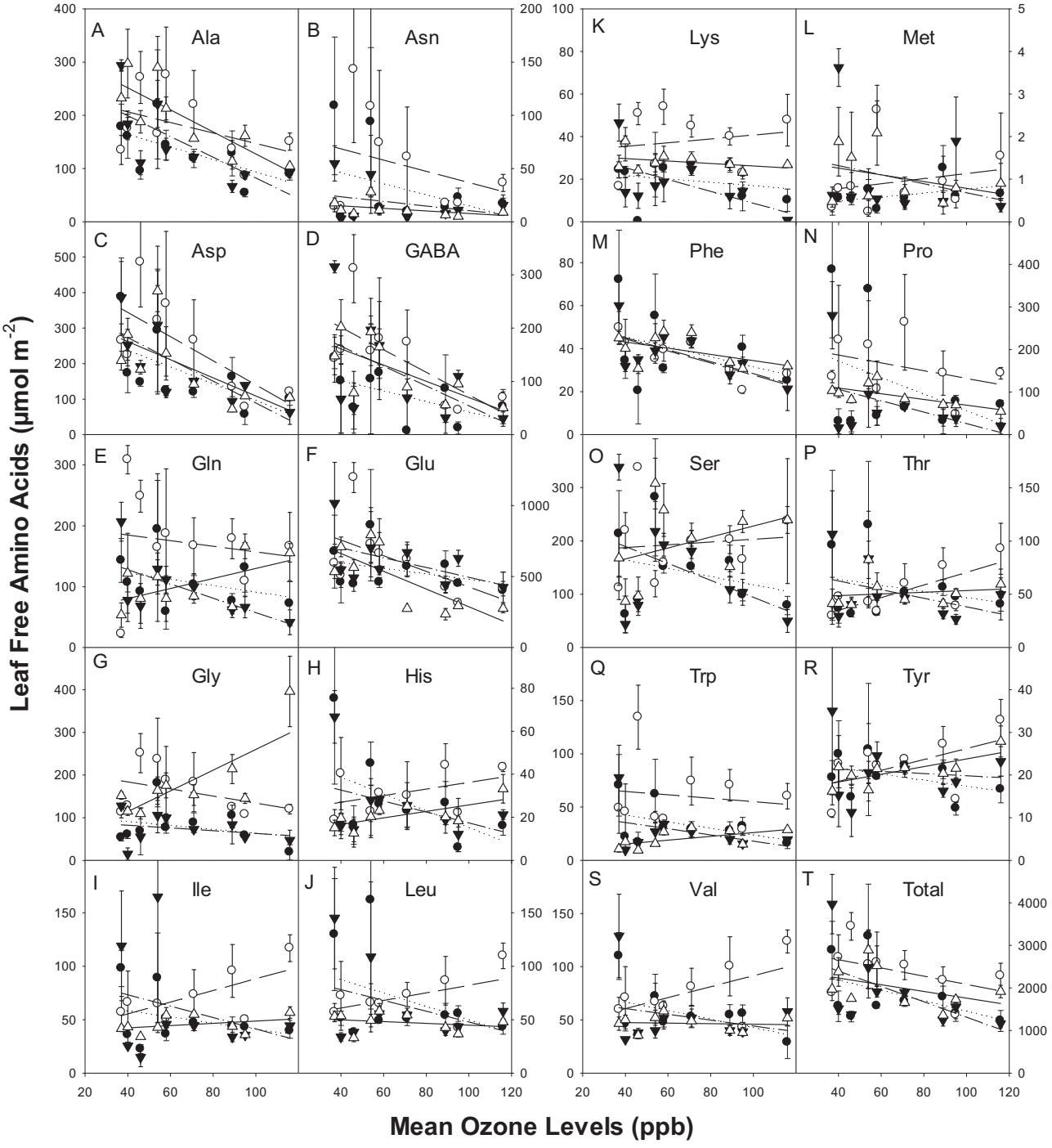

Fig. 10. Amino acids profiling (unit = μmol m^{-2}) in the young leaves (open symbol) and old leaves (closed symbol) of the 2 cultivars (DW, circle; IA, triangle) under various ozone levels at R5 stage. Linear regressions were fit between ozone levels and each of the free amino acids for DW old (dotted line), DW young (dashed line), IA old (dot dash line) and IA young leaves (solid line).

Generally, 3 ppm h for AOT40 is considered as a damage threshold for many crops [5,6]. On average, 11 ppm h for AOT40 would decrease biomass by 10% in various trees and photosynthesis by 10% in Norway spruce (EPA, 2006). Our results show that 7 ppm h for AOT40 would decrease leaf photosynthesis by 10% compared to ambient control (Table 2) which is consistent with ~10% decrease in yield [15], indicating soybean plants are more sensitive to O_3 than various trees. In general, soybean plants have higher stomatal conductance thus higher O_3 influx and therefore higher O_3 damage than various trees.

4.4. Strong correlations among various parameters under various [O_3]

Our results clearly show that elevated O_3 levels in the range from 37 ppb to 116 ppb cause a linear dose-dependent decline in photosynthesis and many metabolites with higher damage at later reproductive stages and in older leaves that is generally cultivar-independent. The correlations among the majority of the parameters of photosynthesis and metabolites are significant under various O_3 levels (Table 3). In addition, photosynthesis, major

Table 3
Correlations (R) among variables at R5 stage The absolute R values greater than 0.2 are significant ($p < 0.05$) N/A, not applicable; ns, not significant.

	%D	%P	%X	A_{sat}	Chiro	Chi	C_i	Citr	Citrate	C_x	ETR	Fru	F'_v/F'_m	Glc	g_m
%P	−0.51														
%X	−0.27	−0.69													
A_{sat}	−0.64	0.96	−0.53												
Chiro	−0.68	0.74	−0.26	0.77											
Chi	−0.80	0.55	0.06	0.66	0.76										
C_i	0.17	−0.85	0.81	−0.71	−0.46	−0.30									
Citr	0.82	−0.66	0.04	−0.77	−0.70	−0.77	0.33								
Citrate	0.19	−0.34	0.22	−0.30	−0.39	−0.29	0.31	0.35							
C_x	−0.78	0.72	−0.14	0.79	0.79	0.94	−0.51	−0.79	−0.32						
ETR	−0.51	1.00	−0.69	0.96	0.74	0.55	−0.85	−0.66	−0.34	0.71					
Fru	−0.11	0.30	−0.25	0.24	0.42	0.19	−0.31	−0.13	−0.37	0.29	0.31				
F'_v/F'_m	−1.00	0.51	0.27	0.64	0.68	0.80	−0.17	−0.82	−0.19	0.78	0.51	0.11			
Glc	−0.01	0.19	−0.20	0.13	0.28	0.08	−0.23	−0.05	−0.36	0.16	0.19	0.96	0.01		
g_m	−0.43	0.81	−0.54	0.87	0.65	0.53	−0.63	−0.66	−0.28	0.65	0.81	0.13	0.43	0.04	
g_s	−0.85	0.55	0.10	0.74	0.69	0.76	−0.11	−0.84	−0.17	0.75	0.55	0.09	0.85	0.01	0.61
J	−0.41	0.89	−0.65	0.87	0.57	0.47	−0.84	−0.56	−0.27	0.68	0.89	0.26	0.41	0.17	0.70
L	0.38	0.36	−0.73	0.15	−0.09	−0.23	−0.75	0.27	−0.20	−0.04	0.36	0.16	−0.38	0.13	0.15
LA	−0.29	−0.15	0.41	−0.13	0.04	0.06	0.20	0.00	0.15	−0.01	−0.15	0.14	0.29	0.21	−0.21
Malate	−0.50	0.91	−0.60	0.90	0.75	0.56	−0.73	−0.63	−0.27	0.69	0.91	0.23	0.50	0.15	0.73
Maltose	−0.21	0.64	−0.53	0.65	0.53	0.25	−0.49	−0.38	−0.20	0.38	0.64	0.31	0.21	0.28	0.54
Myo	−0.32	0.64	−0.44	0.64	0.38	0.29	−0.56	−0.44	−0.03	0.40	0.64	−0.09	0.32	−0.04	0.49
PhiPSII	−0.51	1.00	−0.69	0.96	0.74	0.55	−0.85	−0.66	−0.34	0.72	1.00	0.30	0.51	0.19	0.81
Pinitol	−0.35	0.79	−0.58	0.73	0.71	0.34	−0.64	−0.51	−0.48	0.54	0.79	0.62	0.35	0.53	0.57
qP	−0.31	0.97	−0.82	0.88	0.63	0.41	−0.91	−0.53	−0.34	0.60	0.97	0.31	0.31	0.21	0.76
R_d	0.39	−0.22	−0.09	−0.26	−0.28	−0.28	−0.09	0.32	0.03	−0.17	−0.22	0.04	−0.39	0.03	−0.23
Starch	−0.47	0.83	−0.54	0.84	0.75	0.49	−0.59	−0.57	−0.34	0.64	0.83	0.55	0.47	0.47	0.67
SLW	0.07	0.60	−0.73	0.44	0.33	−0.02	−0.71	−0.11	−0.24	0.16	0.61	0.40	−0.07	0.33	0.42
Suc	−0.49	0.78	−0.46	0.77	0.71	0.47	−0.58	−0.55	−0.23	0.62	0.79	0.60	0.49	0.54	0.53
unkn1	−0.62	0.56	−0.10	0.58	0.63	0.59	−0.38	−0.68	−0.58	0.64	0.56	0.59	0.62	0.53	0.43
V_{cmax}	−0.51	0.93	−0.61	0.94	0.69	0.57	−0.78	−0.69	−0.34	0.76	0.93	0.26	0.51	0.16	0.82

	g_s	J_{max}	L	LA	Malate	Maltose	Myo	PhiPSII	Pinitol	qP	R_d	Starch	SLW	Suc	unkn1
J_{max}	0.49														
L	−0.50	0.40													
LA	0.07	−0.18	−0.24												
Malate	0.56	0.81	0.25	−0.17											
Maltose	0.40	0.63	0.20	−0.19	0.71										
Myo	0.41	0.70	0.19	0.07	0.70	0.64									
PhiPSII	0.55	0.89	0.36	−0.15	0.91	0.64	0.64								
Pinitol	0.39	0.74	0.25	−0.13	0.74	0.70	0.46	0.79							
qP	0.38	0.90	0.52	−0.24	0.87	0.64	0.64	0.97	0.78						
R_d	−0.39	0.11	0.38	−0.30	−0.24	0.00	−0.16	−0.22	−0.01	−0.08					
Starch	0.58	0.73	0.14	−0.06	0.84	0.72	0.50	0.83	0.84	0.77	−0.24				
SLW	−0.09	0.46	0.64	−0.23	0.52	0.35	0.20	0.60	0.56	0.68	0.01	0.53			
Suc	0.55	0.72	0.08	0.11	0.75	0.57	0.55	0.78	0.79	0.73	−0.29	0.88	0.42		
unkn1	0.55	0.48	−0.05	0.08	0.51	0.25	0.21	0.56	0.68	0.46	−0.23	0.58	0.34	0.63	
V_{cmax}	0.58	0.91	0.30	−0.26	0.86	0.66	0.60	0.93	0.78	0.90	−0.06	0.79	0.46	0.72	0.52

non-structural carbohydrates and many N-assimilation related amino acids are highly correlated with soybean yield. The 7% decrease in seed yield in SoyFACE [15] and 5.3% decrease in soybean yield from over 30 independent chamber studies of season long O_3 fumigation [56] agree well with the 6–8% decrease in photosynthesis and major non-structural carbohydrates and metabolites per every 10 ppb increase in O_3 levels.

Rather than carbon translocation into sink tissues through phloem loading as reported previously [57–59], our results indicate that carbon availability limits soybean seed yield under elevated O_3 levels. Both leaf area and leaf photosynthetic capacity decreased under elevated O_3 levels. The decline in photosynthetic capacity is clearly the major factor for soybean yield loss under elevated O_3.

5. Conclusion

Photosynthesis, total non-structural carbohydrate (TNC) levels, and many metabolites and amino acids as well as seed yield are highly correlated to each other and decrease linearly with ozone levels with average decrease by 7% for an increase in O_3 levels by 10 ppb. The average critical O_3 levels that cause 10% decreases in photosynthesis, photosynthetic pigments and TNC are about 50 ppb compared to the ambient control. Loss of seed yield is mainly a result of the loss of photosynthetic capacity that is non-stomatal in origin as well as a shorter growing season due to earlier onset of canopy senescence. Ozone interacts with developmental stages and leaf ages with higher damage at later reproductive stages and in older leaves. In general, both cultivars DW and IA showed similar response to elevated O_3.

Appendix A. Supplementary data

Supplementary data associated with this article can be found, in the online version, at http://dx.doi.org/10.1016/j.plantsci.2014.06.012.

References

[1] E.A. Ainsworth, C.R. Yendrek, S. Sitch, W.J. Collins, L.D. Emberson, The effects of tropospheric ozone on net primary productivity and implications for climate change, Annu. Rev. Plant Biol. 63 (2012) 637–661.

[2] J. Schmidhuber, F.N. Tubiello, Global food security under climate change, Proc. Natl. Acad. Sci. U. S. A. 104 (2007) 19703–19708.
[3] Intergovernmental Panel on Climate Change (IPCC) Fifth Assessment Report, 2009, http://www.ipcc.ch/report/ar5/index.shtml
[4] M. Ashmore, S. Toet, L. Emberson, Ozone – a significant threat to future world food production? New Phytol. 170 (2006) 201–204.
[5] J. Fuhrer, Ozone risk for crops and pastures in present and future climates, Naturwissenschaften 96 (2009) 173–194.
[6] D.L. Mauzerall, X. Wang, Protecting agricultural crops from the effects of tropospheric ozone exposure: reconciling science and standard setting in the United States, Europe and Asia, Ann. Rev. Energy Environ. 26 (2001) 237–268.
[7] X.K. Wang, W.J. Manning, Z.W. Feng, Y.G. Zhu, Ground-level ozone in China: distribution and effects on crop yields, Environ. Pollut. 147 (2007) 394–400.
[8] D. Fowler, I.N. Cape, M. Coyle, C. Flechard, J. Kuylenstierna, K. Hicks, D. Derwent, C. Johnson, D. Stevenson, The global exposure of forests to air pollutants, Water Air Soil Pollut. 116 (1999) 5–32.
[9] D. Fowler, I.N. Cape, M. Coyle, R.I. Smith, A.G. Hjellbrekke, D. Simpson, R.G. Derwent, C.E. Johnson, Modeling photochemical oxidant formation, transport, deposition and exposure of terrestrial ecosystems, Environ. Pollut. 100 (1999) 43–55.
[10] J. Fuhrer, L. Skarby, M.R. Ashmore, Critical levels for ozone effects on vegetation, Eur. Environ. Pollut. 97 (1997) 91–106.
[11] D.R. Ort, E.A. Ainsworth, M. Aldea, et al., SoyFACE: the effects and interactions of elevated [CO_2] and [O_3] on soybean, in: J. Nosberger, S.P. Long, R. Norby, M. Stitt, G.R. Hendrey, H. Blum (Eds.), Managed Ecosystems and CO_2 Case Studies, Processes, and Perspectives, 2006, Ecological Studies, vol. 187, Springer, 2006, pp. 71–86.
[12] P.B. Morgan, T.A. Mies, G.A. Bollero, R.L. Nelson, S.P. Long, Season-long elevation of ozone concentration to projected 2050 levels under fully open-air conditions substantially decreases the growth and production of soybean, New Phytol. 170 (2006) 333–343.
[13] J. Sun, L. Yang, Y. Wang, D.R. Ort, FACE-ing the global change: opportunities for improvement in photosynthetic radiation use efficiency and crop yield, Plant Sci. 177 (2009) 511–522.
[14] P.B. Morgan, C.J. Bernacchi, D.R. Ort, S.P. Long, An in vivo analysis of the effect of season-long open-air elevation of ozone to anticipated 2050 levels on photosynthesis in soybean, Plant Physiol. 135 (2004) 2348–2357.
[15] A.M. Betzelberger, C.R. Yendrek, J. Sun, C.P. Leisnter, R.L. Nelson, D.R. Ort, E.A. Ainsworth, Ozone exposure-response for U.S. soybean cultivars: linear reductions in photosynthetic potential, biomass and yield, Plant Physiol. 160 (2012) 1827–1839.
[16] A. Lavola, R. Julkunen-Tiitto, E. Paakkonen, Does ozone stress change the primary or secondary metabolites of birch (*Betula pendula* Roth.)? New Phytol. 126 (1994) 637–642.
[17] P. Gupta, S. Duplessis, H. White, D.F. Karnosky, F. Martin, G.K. Podila, Gene expression patterns of trembling aspen trees following long-term exposure to interacting elevated CO_2 and tropospheric O_3, New Phytol. 167 (2005) 129–142.
[18] K.M. Gillespie, F. Xu, K.T. Richter, J.M. McGrath, R.J.C. Markelz, D.R. Ort, A.D.B. Leakey, E.A. Ainsworth, Greater antioxidant and respiratory metabolism in field-grown soybean exposed to elevated O_3 under both ambient and elevated CO_2, Plant Cell Environ. 35 (2012) 169–184.
[19] K. Herbinger, C. Then, M. Löw, K. Haberer, M. Alexous, N. Koch, K. Remele, C. Heerdt, D. Grill, H. Rennenberg, K.-H. Haberle, R. Matyssek, M. Tausz, G. Wieser, Tree age dependence and within-canopy variation of leaf gas exchange and antioxidative defense in *Fagus sylvatica* under experimental free-air ozone exposure, Environ. Pollut. 137 (2005) 476–482.
[20] A. Ludwikow, J. Sadowski, Gene networks in plant ozone stress response and tolerance, J. Integr. Plant Biol. 50 (2008) 1256–1267.
[21] J. Sun, J. Zhang, C.T. Larue, S.C. Huber, Decrease in leaf sucrose synthesis leads to increased leaf starch turnover and decreased RuBP regeneration-limited photosynthesis but not Rubisco-limited photosynthesis in *Arabidopsis* null mutants of SPSA1, Plant Cell Environ. 34 (2011) 592–604.
[22] S.P. Long, C.J. Bernacchi, Gas exchange measurements, what can they tell us about the underlying limitations to photosynthesis? Procedures and sources of error, J. Exp. Bot. 54 (2003) 2393–2401.
[23] C.J. Bernacchi, A.R. Portis, H. Nakano, S. von Caemmerer, S.P. Long, Temperature response of mesophyll conductance. Implications for the determination of Rubisco enzyme kinetics and for limitations to photosynthesis in vivo, Plant Physiol. 130 (2002) 1992–1998.
[24] G.D. Farquhar, S. von Caemmerer, J.A. Berry, A biochemical model of photosynthetic CO_2 assimilation in leaves of C3 species, Planta 149 (1980) 78–90.
[25] G.J. Ethier, N.J. Livingston, On the need to incorporate sensitivity to CO_2 transfer conductance into the Farquhar–von Caemmerer–Berry leaf photosynthesis model, Plant Cell Environ. 27 (2004) 137–153.
[26] S.P. Long, J.E. Hallgren, Measurement of carbon dioxide assimilation by plants in the field and the laboratory, in: D.O. Hall, J.M.O. Scurlock, H.R. Bolhar-Nordenkampf, R.C. Leegood, S.P. Long (Eds.), Photosynthesis and Production in a Changing Environment: A Field and Laboratory Manual, Springer, 1993, pp. 129–167.
[27] J. Sun, T.W. Okita, G.E. Edwards, Modification of carbon partitioning, photosynthetic capacity and O_2 sensitivity in *Arabidopsis* plants with low ADP-glucose pyrophosphorylase activity, Plant Physiol. 119 (1999) 267–276.
[28] B. Demmig-Adams, W.W. Adams, D.H. Baker, B.A. Logan, D.R. Bowling, A.S. Verhoeven, Using chlorophyll fluorescence to assess the fraction of absorbed light allocated to thermal dissipation of excess excitation, Physiol. Plant. 98 (1996) 253–264.
[29] P.C. Harley, F. Loreto, G. DiMarco, T.D. Sharkey, Theoretical considerations when estimating the mesophyll conductance to CO_2 flux by analysis of the response of photosynthesis to CO_2, Plant Physiol. 98 (1992) 1429–1436.
[30] C.J. Bernacchi, E.L. Singsaas, C. Pimentel, A.R. Portis Jr., S.P. Long, Improved temperature response functions for models of Rubisco-limited photosynthesis, Plant Cell Environ. 24 (2001) 253–259.
[31] J. Flexas, A. Díaz-Espejo, J. Galmés, R. Kaldenhoff, H. Medrano, M. Ribas-Carbó, Rapid variations of mesophyll conductance in response to changes in CO_2 concentration around leaves, Plant Cell Environ. 30 (2007) 1284–1298.
[32] H.K. Lichtenthaler, Chlorophylls and carotenoids: pigments of photosynthetic biomembranes, Meth. Enzymol. 148 (1987) 350–382.
[33] J. Sun, K.M. Gibson, O. Kiirats, T.W. Okita, G.E. Edwards, Interactions of nitrate and CO_2 enrichment on growth. Carbohydrates, and Rubisco in *Arabidopsis* starch mutants. Significance of starch and hexose, Plant Phyiol. 130 (2002) 1573–1583.
[34] M.H. Oh, J. Sun, D.H. Oh, R.E. Zielinski, S.D. Clouse, S.C. Huber, Enhancing *Arabidopsis* leaf growth by engineering the BRASSINOSTEROID INSENSITIVE1 receptor kinase, Plant Physiol. 157 (2011) 120–131.
[35] L.S. Evans, K. Albury, N. Jennings, Relationship between anatomical characteristics and ozone sensitivity of leaves of several herbaceous dicotyledonous plant species at great Smoky Mountains National Park, Environ. Exp. Bot. 36 (1996) 413–420.
[36] G. Wieser, K. Hecke, M. Tausz, K.H. Häberle, T.E.E. Grams, R. Matyssek, The role of antioxidative defense in determining ozone sensitivity of Norway spruce (*Picea abies* (L.) Karst.) across tree age: implications for the sun- and shade-crown, Phyton 42 (2002) 245–253.
[37] S.P. Long, S.L. Naidu, Effects of oxidants at the biochemical, cell and physiological levels with particular reference to ozone, in: J.N.B. Bell, M. Treshow (Eds.), Air Pollution and Plants, 2nd ed., J. Wiley, London, 2002, pp. 69–88.
[38] G. Torsethaugen, E.J. Pell, S.M. Assmann, Ozone inhibits guard cell K+ channels implicated in stomatal opening, Proc. Natl. Acad. Sci. U. S. A. 96 (1999) 13577–13582.
[39] C.R. Warren, M. Löw, R. Matyssek, M. Tausz, Internal conductance to CO_2 transfer of adult *Fagus sylvatica*: variation between sun and shade leaves and due to free-air ozone fumigation, Environ. Exp. Bot. 59 (2007) 130–138.
[40] V. Velikova, T. Tsonev, P. Pinelli, G.A. Alessio, F. Loreto, Localized ozone fumigation system for studying ozone effects on photosynthesis, respiration, electron transport rate and isoprene emission in field-grown Mediterranean species, Tree Physiol. 25 (2005) 1523–1532.
[41] H. Eichelmann, V. Oja, B. Rasulov, E. Padu, I. Bichele, H. Pettai, T. Möls, I. Kasparova, E. Vapaavuori, A. Laisk, Photosynthetic parameters of birch (*Betula pendula* Roth.) leaves growing in normal and CO_2- and O_3-enriched atmospheres, Plant Cell Environ. 27 (2004) 479–495.
[42] M.D. Flowers, E.L. Fiscus, K.O. Burkey, F.L. Booker, J.-J.B. Dubois, Photosynthesis, chlorophyll fluorescence, and yield of snap bean (*Phaseolus vulgaris* L.) genotypes differing in sensitivity to ozone, Environ. Exp. Bot. 61 (2007) 190–198.
[43] T.D. Sharkey, O_2-insensitive photosynthesis in C3 plants: its occurrence and a possible explanation, Plant Physiol. 78 (1985) 71–75.
[44] J.G. Streeter, D.G. Lohnes, R.J. Fioritto, Patterns of pinitol accumulation in soybean plants and relationships to drought tolerance, Plant Cell Environ. 24 (2001) 429–438.
[45] L. Guidi, E. Degl'Innocenti, F. Martinelli, M. Piras, Ozone effects on carbon metabolism in sensitive and insensitive *Phaseolus cultivars*, Environ. Exp. Bot. 66 (2009) 117–125.
[46] V. Fontaine, M. Cabane, P. Dizengremel, Regulation of phosphoenolpyruvate carboxylase in *Pinus halepensis* needles submitted to ozone and water stress, Physiol. Plant. 117 (2003) 445–452.
[47] W. Landolt, M.S. Gunthardt-Goerg, I. Pfenninger, W. Eining, R. Hampp, S. Maurer, R. Matyssek, Effect of fertilization on ozone induced changes in the metabolism of birch leaves (*Betula pendula*), New Phytol. 137 (1997) 389–397.
[48] P. Dizengremel, Effects of ozone on the carbon metabolism of forest trees, Plant Physiol. Biochem. 39 (2001) 729–742.
[49] Z. Feng, K. Kobayashi, E.A. Ainsworth, Impact of elevated ozone concentration on growth, physiology, and yield of wheat (*Triticum aestivum* L.): a meta-analysis, Global Change Biol. 14 (2008) 2696–2708.
[50] D. Tingey, Ozone induced alterations in the metabolite pools and enzyme activities of plants, in: M. Dugger (Ed.), Air Pollution Effects on Plant Growth, ACS Symposium Series, American Chemical Society, Washington, DC, 1974.
[51] I. Janzik, S. Preiskowski, H. Kneifel, Ozone has dramatic effects on the regulation of the prechorismate pathway in tobacco (*Nicotiana tabacum* L. cv. Bel W3), Planta 223 (2005) 20–27.
[52] N. Bouche, H. Fromm, GABA in plants: just a metabolite? Trends Plant Sci. 9 (2004) 110–115.
[53] P.D. Hare, W.A. Cress, Metabolic implications of stress-induced proline accumulation in plants, Plant Growth Regul. 21 (1997) 79–102.
[54] T.C. Williams, L.J. Sweetlove, R.G. Ratcliffe, Capturing metabolite channeling in metabolic flux phenotypes, Plant Physiol. 157 (2011) 981–984.
[55] M. Szecowka, R. Heise, T. Tohge, A. Nunes-Nesi, D. Vosloh, J. Huege, R. Feil, J. Lunn, Z. Nikoloski, M. Stitt, et al., Metabolic fluxes in an illuminated *Arabidopsis rosette*, Plant Cell 25 (2013) 694–714.

[56] M.R. Ashmore, Effects of oxidants at the whole plant and community level, in: J.N.B. Bell, M. Treshow (Eds.), Air Pollution and Plants, 2nd ed., J. Wiley, London, 2002.
[57] C.L. Mulchi, L. Slaughter, M. Saleem, E.H. Lee, R. Pausch, R. Rowland, Growth and physiological-characteristics of soybean in open-top chambers in response to ozone and increased atmospheric CO_2, Agric. Ecosyst. Environ. 38 (1992) 107–118.
[58] D.A. Grantz, J.F. Farrar, Acute exposure to ozone inhibits rapid carbon translocation from source leaves of Pima Cotton, J. Exp. Bot. 50 (1999) 1253–1262.
[59] U. Meyer, B. Kollner, J. Willenbrink, G.H.M. Krause, Physiological changes on agricultural crops induced by different ambient ozone exposure regimes. 1. Effects on photosynthesis and assimilate allocation in spring wheat, New Phytol. 136 (1997) 645–652.